



Research paper

Novel S1P₁ receptor agonists – Part 4: Alkylaminomethyl substituted aryl head groups

Cyrille Lescop^{*}, Claus Müller, Boris Mathys, Magdalena Birker, Ruben de Kanter, Christopher Kohl, Patrick Hess, Oliver Nayler, Markus Rey, Patrick Sieber, Beat Steiner, Thomas Weller, Martin H. Bolli

Drug Discovery Chemistry, Actelion Pharmaceuticals Ltd., Gewerbestrasse 16, CH-4123 Allschwil, Switzerland

ARTICLE INFO

Article history:

Received 26 August 2015

Received in revised form

17 December 2015

Accepted 18 March 2016

Available online 23 March 2016

Keywords:

S1P₁ receptor agonist

Immunomodulator

Lymphocyte count

Aminomethyl pyridine

Aminomethyl benzene

Aminomethyl thiophene

Phototoxicity

ABSTRACT

In a previous communication we reported on the discovery of alkylamino pyridine derivatives (e.g. **1**) as a new class of potent, selective and efficacious S1P₁ receptor (S1PR₁) agonists. However, more detailed profiling revealed that this compound class is phototoxic *in vitro*. Here we describe a new class of potent S1PR₁ agonists wherein the exocyclic nitrogen was moved away from the pyridine ring (e.g. **11c**). Further structural modifications led to the identification of novel alkylaminomethyl substituted phenyl and thienyl derivatives as potent S1PR₁ agonists. These new alkylaminomethyl aryl compounds showed no phototoxic potential. Based on their *in vivo* efficacy and ability to penetrate the brain, the 5-alkylaminomethyl thiophenes appeared to be the most interesting class. Potent and selective S1PR₁ agonist **20e**, for instance, maximally reduced the blood lymphocyte count (LC) for 24 h after oral administration of 10 mg/kg to rat and its brain concentrations reached >500 ng/g over 24 h.

© 2016 Elsevier Masson SAS. All rights reserved.

1. Introduction

Sphingosine-1 phosphate (S1P, Fig. 1) is a bioactive phospholipid produced by sphingosine kinase-mediated phosphorylation of sphingosine, a metabolite of ceramide. S1P is involved in a number of pathological conditions such as autoimmune diseases, cancer, fibrosis, atherosclerosis, diabetes and osteoporosis [1–9]. These observations confirm the critical role of S1P in cellular processes

Abbreviations used: BuLi, *n*-butyl lithium; CC, column chromatography; DCM, dichloromethane; DIPEA, diisopropylethylamine; DEAD, diethyl azodicarboxylate; DMF, dimethylformamide; EA, ethyl acetate; EDC, 1-ethyl-3-(3-dimethylaminopropyl)carbodiimide; fu_{mic}, unbound fraction in microsomal incubations; fu_p, unbound fraction in plasma; HOBt, *N*-hydroxybenzotriazole; LC, lymphocyte count; LC-MS, (high pressure) liquid chromatography combined with mass spectrometry; MeCN, acetonitrile; MeOH, methanol; NMP, *N*-methylpyrrolidine; PK, pharmacokinetics; PPh₃, triphenylphosphine; RLM, rat liver microsomes; SAR, structure-activity relationship; S1P, sphingosine 1-phosphate; S1PR₁, sphingosine 1-phosphate 1 receptor; S1PR₃, sphingosine 1-phosphate 3 receptor; TBTU, O-(benzotriazol-1-yl)-*N,N,N',N'*-tetramethyluronium tetrafluoroborate; TFA, trifluoroacetic acid; THF, tetrahydrofuran.

^{*} Corresponding author.

E-mail address: cyrille.lescop@actelion.com (C. Lescop).

[10–12] as well as tissue and organ function such as cell growth [13], vascular development [14], immune cell trafficking [15–18], cardiac function and inflammation [5] to name a few. Regulation of these functions is primarily orchestrated by the interaction of S1P with a family of five G-protein coupled receptors known as S1PR_{1–5} [10,19–21]. The S1PR_{1–3} are widely expressed in almost all organs, while S1PR₄ is predominantly expressed on lymphoid and hematopoietic tissues and S1PR₅ is primarily located in the spleen and in the white matter of the central nervous system. Over the last decade, the role of the S1P–S1P₁ receptor signaling axis in immune-mediated diseases has been studied in detail [4,22,23]. The S1P₁ receptor subtype plays a central role in the control of lymphocyte migration. Upon activation in the lymph node by an antigen presenting cell, lymphocytes up-regulate S1P₁ receptor expression and are thus able to sense the concentration gradient of S1P that exists between lymph and blood. By migrating along this gradient, lymphocytes exit the lymph nodes and secondary lymphoid organs, reach the systemic circulation and finally the intruder and target tissue. Understanding of the mechanism of action of S1PR₁ agonists has grown rapidly with the discovery that fingolimod (FTY720, Fig. 1) – the first-in-class oral drug approved for the treatment of relapsing remitting multiple sclerosis [24] – is

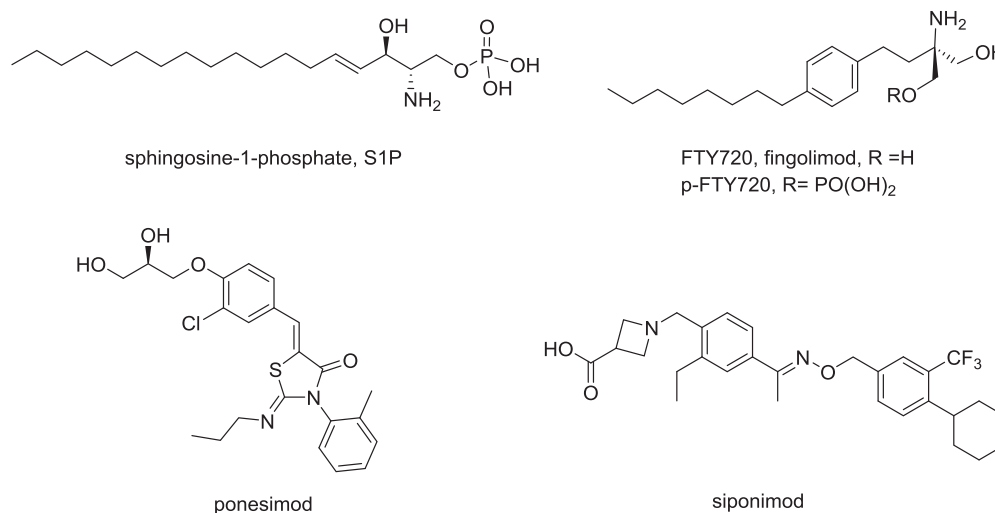


Fig. 1. Structures of sphingosine 1-phosphate, FTY720 (fingolimod), p-FTY720, ponesimod and siponimod

phosphorylated *in vivo* by sphingosine kinases to become a potent, non-selective S1PR agonist, p-FTY720 (Fig. 1) [25–27]. Activation of the S1P₁ receptor by a synthetic S1PR₁ agonist leads to receptor internalization and thus desensitization of the lymphocytes toward the S1P gradient. As a consequence lymphocytes lose their ability to exit the lymph node and can no longer reach sites of inflammation in the tissue. Mechanistically, synthetic S1PR₁ agonists therefore act as functional antagonists [28–31]. Disrupted trafficking of activated lymphocytes by down-regulation of S1P₁ receptors using synthetic S1PR₁ modulators represents an attractive concept to treat a variety of lymphocyte dependent immune diseases such as multiple sclerosis, Crohn's disease, systemic lupus erythematosus, or psoriasis [1,15,32]. Over the last few years, numerous synthetic S1PR₁ agonists have been identified as a result of dedicated drug discovery efforts [33–35].

In addition to the peripheral immunomodulatory action of S1PR₁ agonists, more recent studies identified activation of the S1P₁, S1P₃ or S1P₅ receptors on neural cells like astrocytes and oligodendrocytes to lead to beneficial effects [19]. Following these arguments, brain penetration of a synthetic S1PR₁ agonist may be contributing to the compound's efficacy in CNS related diseases such as multiple sclerosis [36–39].

Several publications showed that activation of the S1P₃ receptor is associated with cardiovascular liabilities in rodents such as heart rate reduction, hypertension and vaso-constriction [40–44]. On the other hand, in the absence of data with selective S1PR₂ and S1PR₄ modulators, the benefit of modulating S1PR₂ and S1PR₄ remains unclear [45]. Therefore, more recent research focused on the identification and exploration of selective S1PR₁ agonists in order to improve the safety profile of pan-S1PR agonist which induces transient heart rate reduction [35,46–51]. Lately, some of these more selective compounds such as ponesimod [52], siponimod [53], and RPC1063 [54] (structure not published) (Fig. 1) successfully completed phase II clinical trials in relapsing remitting multiple sclerosis [55]. However, transient heart rate reduction was not totally eliminated implying that the S1P₁ receptor is involved in the regulation of the heart rate in humans [56–58].

In a previous communication we reported on the discovery of alkyl-amino pyridine derivatives such as **1** as a new class of selective and efficacious S1PR₁ agonists (Fig. 2) [59]. However, more detailed profiling of this alkylamino pyridine-based series revealed that this compound class is phototoxic *in vitro*. The potential for phototoxicity was assessed *in vitro* using the 3T3 Neutral Red

Uptake (NRU) Phototoxicity assay. This assay measures cell viability by comparing the concentration-dependent reduction in NRU by normal BALB/c 3T3 mouse fibroblasts after exposure to a test compound in the presence and absence of UVA light [60,61]. The cytotoxicity IC₅₀ values obtained in the presence and absence of light are then used to calculate a photo-irritancy factor (PIF). A PIF value greater than 2.5 is indicative of phototoxic potential [62]. All tested alkylamino pyridine derivatives shown in Fig. 2 were above the cut-off value of 2.5, with compounds **1–3** exhibiting a PIF > 200. Planar and conjugated polycyclic structures containing heteroatoms are considered a structural alert for drug-induced phototoxicity [63,64], as they can absorb UV light and generate an electronically excited species that could cause biological damage. We therefore systematically evaluated other related pyridine series in the 3T3 NRU phototoxicity assay. We discovered that the dialkyl pyridine series was devoid of this property as illustrated by example **4** [59] and we hypothesized that the alkylamino pyridine moiety is the major driver of this unwanted effect (Fig. 2). We then speculated that introducing a methylene linker between the pyridine and the amino group would reproduce the clean profile of the dialkyl pyridine series while keeping clogP ≤ 3.0. Indeed, first examples such as compounds **5** and **6** were clean in the cellular phototoxicity assay (PIF < 2.5). Even though compounds **5** and **6** were less potent with EC₅₀ values on S1PR₁ of 45 nM and 110 nM, respectively, they were still attractive because of their reduced lipophilicity compared to compound **4** (clogP of 2.15, 3.06 and 3.71 respectively). These results prompted us to investigate the scope of various alkylaminomethyl substituted aryl series in more detail. In this article we describe the discovery of potent alkylaminomethyl pyridine, benzene and thiophene based S1PR₁ agonists with the following profile: the compound is very potent on S1PR₁ (EC₅₀ < 5 nM) with a high selectivity against S1PR₃ (≥ 100-fold), has a clogP ≤ 3, is devoid of phototoxicity potential (PIF < 2.5), and shows maximal lymphocyte count reduction for at least 24 h at an oral dose of 10 mg/kg in the Wistar rat.

2. Results and discussion

2.1. Synthesis

Alkylaminomethyl substituted pyridine derivatives **5** and **11a-e** were prepared as outlined in Scheme 1. Like in previous series [59,65,66] several side chains at position 4 of the phenyl ring have

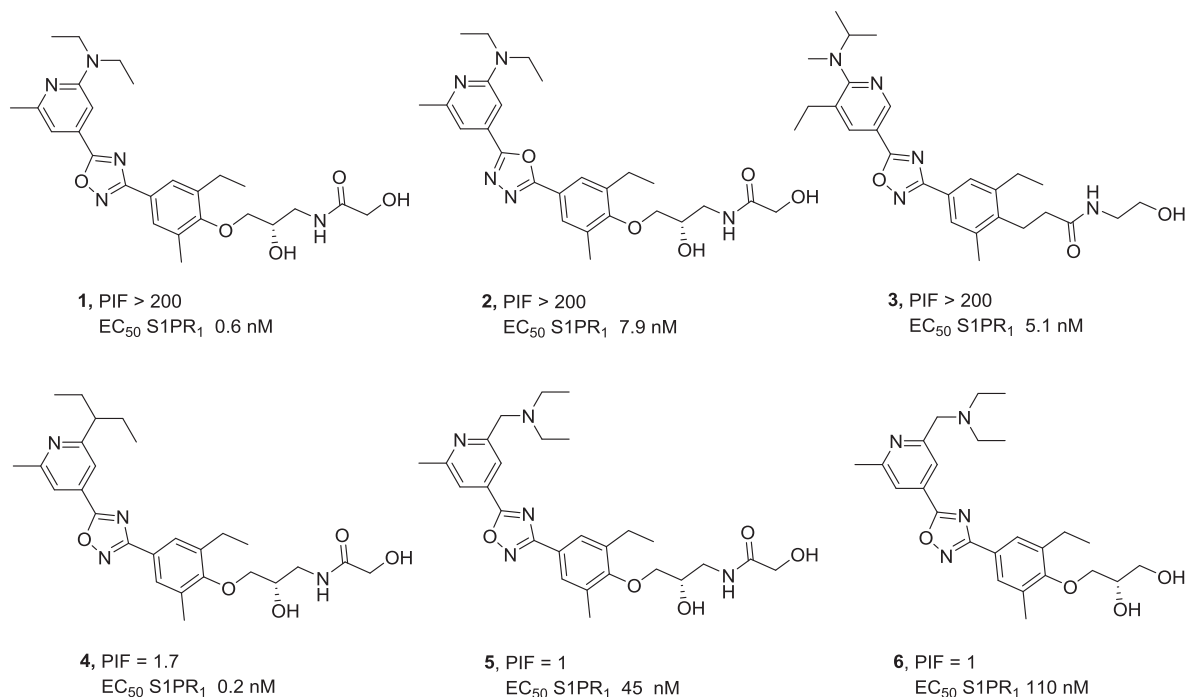
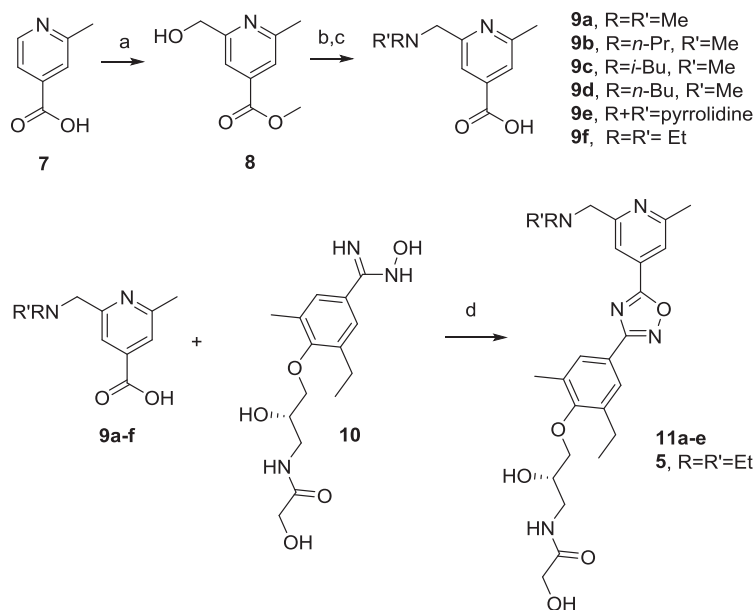


Fig. 2. Photo-irritancy factor (PIF) and EC_{50} S1PR₁ (GTPγS) values in six related pyridine series.

been studied and many led to potent compounds (data not shown). The glycolamide moiety shown in **5** appeared to be one of the most interesting side chains in terms of affinity and selectivity for the S1P₁ receptor and was selected to discuss the structure activity

relationship of the present series. The key intermediate of the synthesis is the 2-(hydroxymethyl)-6-methylisonicotinic acid methyl ester **8**. First, commercially available 2-methylpyridine-4-carboxylic acid **7** was converted to its methyl ester which was



^aReagents and conditions: (a) (1) H₂SO₄, MeOH, 65 °C, 24 h ; (2) (NH₄)₂S₂O₈, H₂O, 65 °C, 10 h, 62%; (b) MsCl, DIPEA, DCM, rt, 1 h, 96% crude; (c) RR'NH, MeCN, 40 °C, 3-16 h then 2N LiOH, 1 h, 20-52%; (d) (1) TBTU or EDC.HCl/HOBt, DIPEA, DMF, rt, 1-2 h; (2) dioxane or DMF 80-110 °C, 2-48 h; 1-48%.

Scheme 1. Preparation of 2-alkylaminomethyl substituted pyridine derivatives^a.

then reacted with ammonium persulfate under Minisci conditions [67] to afford 2-(hydroxymethyl)pyridine derivative **8**. The hydroxymethyl pyridine **8** was reacted with methanesulfonyl chloride to provide the corresponding mesylate intermediate which, after nucleophilic substitution with various amines and subsequent saponification, gave the corresponding 2-aminomethyl-6-methylisonicotinic acids **9a-f**. These acids were coupled with (*S*)-*N*-(3-(2-ethyl-4-(*N*-hydroxycarbamimidoyl)-6-methylphenoxy)-2-hydroxypropyl)-2-hydroxyacetamide **10** [59]. Typical coupling conditions involved TBTU or EDC.HCl/HOBt as activating agents. Subsequent cyclization of the hydroxyamidine ester intermediate at 80–100 °C furnished the desired oxadiazole compounds **5** and **11a-e** in moderate yield. We usually obtained better yields in the cyclization step when all reagents were added at once rather than in a sequential manner allowing the activation of the pyridine carboxylic acids **9a-f**. However, we did not further optimize this procedure as this synthesis delivered sufficient material for a first evaluation of the desired target compounds.

Related alkylaminomethyl aryl series were prepared from the corresponding formyl aryl carboxylic acids. Thus, the synthesis of the 3-alkylaminomethyl benzene series (**14a-s**) was carried out as depicted in Scheme 2. As in the pyridine series, the alkylaminomethyl group is in *meta* position to the oxadiazole linker. 3-Formyl benzoic acids **12a-g** were prepared according to literature procedures (see Supplementary Material), and were then coupled with (*S*)-*N*-(3-(2-ethyl-4-(*N*-hydroxycarbamimidoyl)-6-methylphenoxy)-2-hydroxypropyl)-2-hydroxyacetamide **10** using EDC.HCl and HOBt, and cyclized at 80–110 °C in DMF or dioxane to give the oxadiazole intermediates **13a-g**. A final reductive amination of benzaldehydes **13a-g** using either sodium cyanoborohydride or sodium triacetoxyborohydride as the reducing agent provided the corresponding 3-aminomethyl benzene derivatives **14a-s** in moderate yield.

In the benzene series, we also investigated compounds **17a-o** wherein the aminomethyl residue was moved to the *para* position

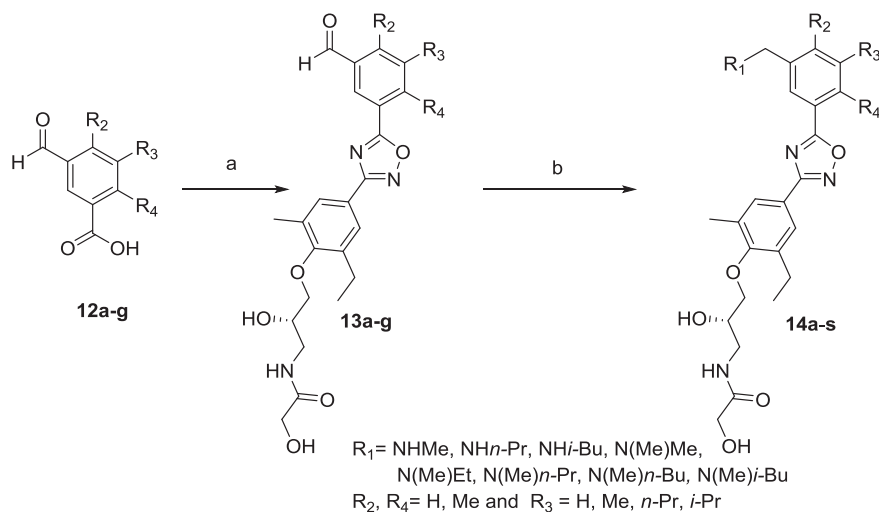
with respect to the oxadiazole. As outlined in Scheme 3, derivatives **17a-o** were synthesized from the corresponding 4-formyl benzoic acids **15a-e** following a similar “coupling-cyclization-reductive amination” sequence. The 4-formyl benzoic acids **15a-e** were commercially available or synthesized according to literature procedures [68,69]. For details on the synthesis of **15a-e** see Supplementary Material.

The same strategy was applied to the synthesis of the 5-alkylaminomethyl thiophene derivatives **20a-s** (Scheme 4). 5-Formylthiophene-2-carboxylic acids **18a-d** [70,71] were coupled with (*S*)-*N*-(3-(2-ethyl-4-(*N*-hydroxycarbamimidoyl)-6-methylphenoxy)-2-hydroxypropyl)-2-hydroxyacetamide **10** using EDC.HCl and HOBt as activating agents and the resulting hydroxyamidine ester intermediates were then cyclized at 80–100 °C to the oxadiazole derivatives **19a-d**. Reductive amination with the appropriate amine in the presence of sodium cyanoborohydride or sodium triacetoxyborohydride furnished the desired target compounds **20a-s** usually in good yield.

In previous work we demonstrated that the chiral integrity is maintained during the above described coupling-cyclization procedure [59]. This was verified exemplarily by subjecting the (*S*)-enantiomer **20e** and its (*R*)-enantiomer **20e'** (prepared from (*R*)-*N*-(3-(2-ethyl-4-(*N*-hydroxycarbamimidoyl)-6-methylphenoxy)-2-hydroxypropyl)-2-hydroxyacetamide **10'**, see Supplementary Material) to HPLC using a chiral stationary phase (Chiralpak AD-H 250 × 4.6 mm ID, 5 μM). Compounds **20e** and **20e'** each displayed a single peak with a retention time of 16.8 and 12.4 min, respectively, and showed no sign of racemization.

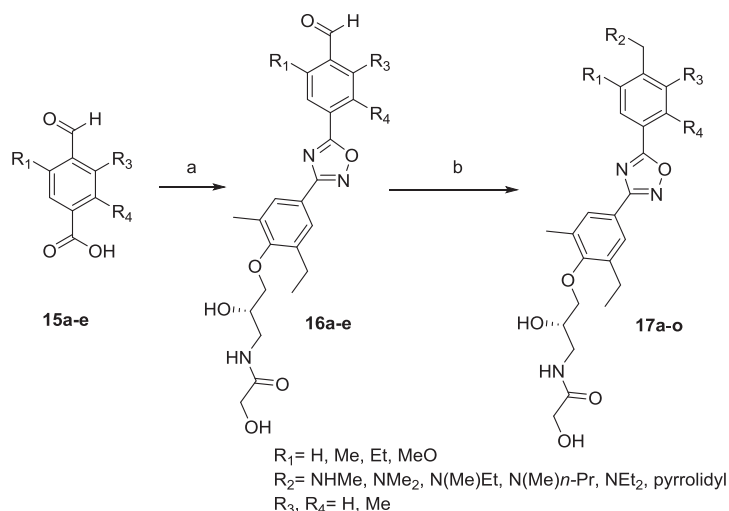
2.2. In vitro SAR discussion

For the different alkylaminomethyl substituted aryl series discussed here, affinity and selectivity for the S1P₁ receptor were determined using a GTPγS binding assay with membranes containing the S1P₁ or the S1P₃ receptor. In the 2-alkylaminomethyl



^aReagents and conditions: (a) (1) (*S*)-*N*-(3-(2-ethyl-4-(*N*-hydroxycarbamimidoyl)-6-methylphenoxy)-2-hydroxypropyl)-2-hydroxyacetamide **10**, EDC.HCl, HOBt, DMF, rt, 2-18 h; (2) dioxane or DMF, 80-110 °C, 2-48 h, 25-61%; (b) primary or secondary amine, NaBH₃CN, MeOH/NMP or NaBH(OAc)₃, HOAc, DCM, NMP, rt, 18 h, 23-67%. For the structure of compounds **12a-g**, **13a-g**, and **14a-s** see Table 2 and Supplementary Material.

Scheme 2. Preparation of 3-alkylaminomethyl benzene derivatives^a.

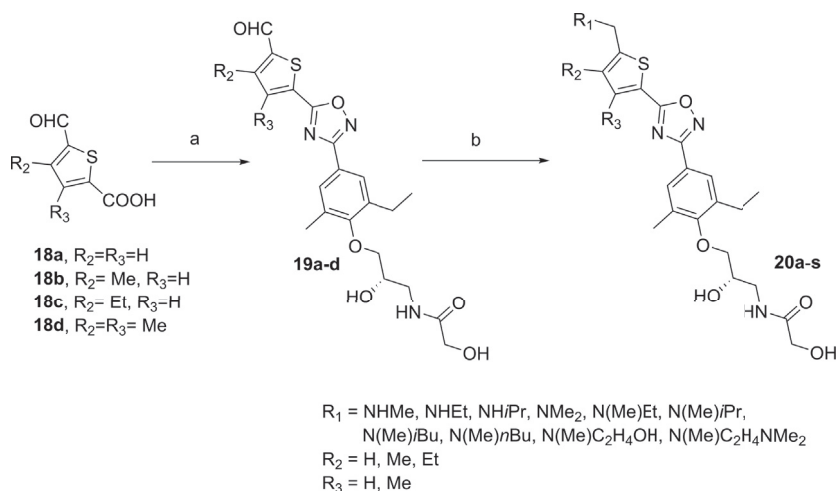


^aReagents and conditions: (a) (S)-N-(3-(2-ethyl-4-(N-hydroxycarbamimidoyl)-6-methylphenoxy)-2-hydroxypropyl)-2-hydroxyacetamide **10**, EDC.HCl, HOBT, DMF, rt, 1-2 h; (2) dioxane or DMF, 80-110 °C, 2-48 h, 26-67% ; (b) primary or secondary amine, NaBH₃CN or NaBH(OAc)₃, HOAc, DCM/NMP, rt, 18 h, 17-93%. For the structure of compounds **15a-e**, **16a-e**, and **17a-o** see Table 3 and Supplementary Material.

Scheme 3. Preparation of 4-alkylaminomethyl benzene derivatives^a.

substituted pyridine series a selection of representative compounds (**5**, **11a-e**) is compiled in Table 1. Compound **11a** displayed an EC₅₀ at S1PR₁ of 40 nM demonstrating that the S1PR₁ receptor can accommodate a basic moiety in the head group. In this compound class, the potency on S1PR₁ could be improved by increasing the size of the dialkylamino residue. For example replacing one methyl group

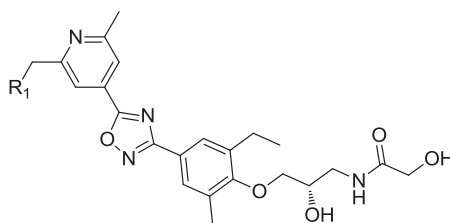
of the dimethylamino derivative **11a** by an *n*-propyl, an *n*-butyl or an *iso*-butyl group furnished compounds **11b**, **11d** and **11c** with very high affinity for the S1PR₁ receptor (EC₅₀ S1PR₁ = 8.5, 4.3 and 3.2 nM, respectively). Interestingly, increasing the size of the second alkyl group attached to the nitrogen led to clearly less potent compounds. This is illustrated with the diethylaminomethyl pyridine **5**



^aReagents and conditions: (a) (1) (S)-N-(3-(2-ethyl-4-(N-hydroxycarbamimidoyl)-6-methylphenoxy)-2-hydroxypropyl)-2-hydroxyacetamide **10**, EDC.HCl, HOBT, DMF, rt 1-2 h; (2) dioxane or DMF, 80-110 °C, 2-48 h, 46-84%; (b) primary or secondary amine, NaBH₃CN or NaBH(OAc)₃, DCM, NMP, HOAc, rt, 18-72 h, 4-88%. For the structure of compounds **19a-d** and **20a-s** see Table 4 and Supplementary Material.

Scheme 4. Preparation of 5-alkylaminomethyl substituted thiophene derivatives^a.

Table 1
SAR of the 2-aminomethyl pyridine series.



Compd	R ₁	clogP	EC ₅₀ S1PR ₁ ^a [nM]	EC ₅₀ S1PR ₃ ^a [nM]	Selectivity ^b
11a		1.33	40	>10000	>250
11b		2.20	8.5	870	102
11c		2.41	3.2	560	175
11d		2.65	4.3	1500	349
5		2.15	45	8100	180
11e		2.13	95	>10000	>105

^a EC₅₀ values measured in a GTPγS assay using membranes of CHO cells expressing either S1PR₁ or S1PR₃; EC₅₀ values are the geometric mean of at least three independent measurements in duplicate.

^b Selectivity against S1PR₃ calculated as the ratio EC₅₀ S1PR₃/EC₅₀ S1PR₁.

and the pyrrolidine-methyl derivative **11e**. Usually, the 2-alkylaminomethyl substituted pyridine series exhibited a more than 100-fold selectivity against the S1P₃ receptor.

Next, we extended our studies to compounds wherein the pyridine was replaced by a benzene ring to evaluate the influence of a more lipophilic ring on the receptor affinity. As shown with the examples listed in Table 2, the aminomethyl residue alone is sufficient to keep a reasonable logP value. While the benzene derivative **14a** was more potent on S1PR₁ when compared to its pyridine analog **11a**, the benzene derivative **14e** showed a similar affinity for S1PR₁ as its pyridine analog **11c**. Increasing the size of the alkyl chain attached to the amino group (compounds **14a–e**) left the affinity for S1PR₁ largely unchanged but clearly increased the compound's potency on S1PR₃. On the other hand, increasing the size of the R₃ residue resulted in potent dual S1PR_{1/3} agonists (**14f–h**) – an observation we already made in a related series [59].

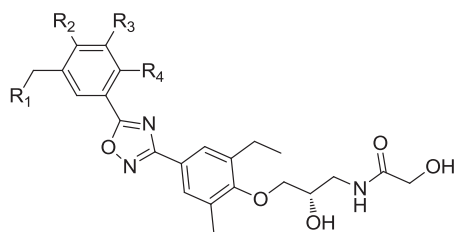
Replacing the tertiary amine by a secondary amine (**14i**) increased the selectivity against the S1P₃ receptor (140-fold) but at the cost of a 7-fold decrease in potency on the S1P₁ receptor. Compounds missing an additional alkyl residue at the phenyl ring (compare **14j** to **14a**, **14k** to **14c** and **14l** to **14e**) were clearly less potent on S1PR₁ and showed no measurable affinity for S1PR₃. Moving the methyl substituent from the *meta* (R₃) to the *ortho* position (R₂) with respect to the aminomethyl substituent led to a significant loss in affinity for the S1PR₁ but affected the potency on the S1PR₃ only moderately (compare e.g. **14n** vs **14b**, **14o** vs **14c**, **14p** vs **14d**, etc.). A similar effect was observed when the R₃ methyl group was moved to the *para* (R₄) position. Compound **14s** was more than 200 times less potent on S1PR₁ when compared to its regio-isomer **14e**.

Table 3 compiles some representatives of the 4-aminomethyl benzene series. In general, the SAR of the 4-aminomethyl series is similar to the one of the 3-aminomethyl derivatives. As illustrated

with the dimethylamino compound **17a**, also this substitution pattern furnished compounds with low nanomolar affinity for S1PR₁ and good selectivity against S1PR₃. Increasing the size of the alkyl group attached to the benzylic nitrogen (compounds **17a–f**) had little effect on the compound's potency on S1PR₁ and produced a slight trend towards higher affinity for S1PR₃. As illustrated with the two pairs **17d/17g**, and **17h/17i**, replacing the tertiary amine by a secondary amine resulted in a significant potency loss on both S1PR₁ and S1PR₃. Similarly, removing the methyl group attached as R₁ to the benzene head (**17h** vs **17a**) led to a clear reduction in potency. Adding a methyl group in the second *ortho* position to the aminomethyl substituent (R₃, compound **17j**) reduced the compound's affinity for S1PR₁ as well. A methyl group in *meta* to the aminomethyl group (R₄) was also detrimental (compound **17k**). As illustrated with the pairs **17a/17l**, **17b/17m**, **17e/17n**, and **17f/17o**, increasing the size of the alkyl group in R₁ improved the compound's affinity for S1PR₁ and S1PR₃ about 10-fold, while providing a 100-fold selectivity against S1PR₃.

In a last series we replaced the benzene ring by a thiophene. The SAR of this class is illustrated with the compounds listed in Table 4. In general the thiophene derivatives were often significantly more potent on S1PR₁ when compared to the corresponding analogs of the 3- and 4-aminomethyl benzene series. For instance, thiophenes **20a**, **20b**, **20c**, **20d**, and **20e**, are more than 150 times more potent on S1PR₁ when compared to the corresponding 3-aminomethyl benzenes **14m**, **14n**, **14o**, **14p**, and **14q**, respectively. In comparison to the 4-aminomethyl benzenes **17a**, **17b**, **17c**, and **17d** the thiophenes **20a**, **20b**, **20d**, and **20e** are about 10 times more potent. As already observed in the two benzene series, the affinity for S1PR₁ did not change in going from the dimethylamino derivative **20a** to the much bulkier isobutyl-methylamino analog **20e**, and there was no clear SAR for compounds **20a** to **20e** with respect to potency on S1PR₃. Interestingly, while an alcohol function attached

Table 2
SAR of the 3-aminomethyl benzene series.



Compd	R ₁	R ₂	R ₃	R ₄	clogP	EC ₅₀ S1PR ₁ ^a [nM]	EC ₅₀ S1PR ₃ ^a [nM]	Selectivity ^b
14a		H	Me	H	2.23	8.0	2000	250
14b		H	Me	H	2.63	3.6	1250	347
14c		H	Me	H	3.09	4.1	380	93
14d		H	Me	H	3.54	2.6	425	163
14e		H	Me	H	3.31	2.1	100	48
14f		H	Et	H	3.72	1.1	8.0	7
14g		H	<i>n</i> -Pr	H	4.18	2.8	3.5	<2
14h		H	<i>i</i> -Pr	H	4.15	1.1	1.4	<2
14i		H	Me	H	3.04	15	2100	140
14j		H	H	H	1.62	190	>10000	>53
14k		H	H	H	2.47	305	>10000	>33
14l		H	H	H	2.69	230	>10000	>43
14m		Me	H	H	2.22	385	>10000	>26
14n		Me	H	H	2.63	285	9000	32
14o		Me	H	H	3.09	305	4300	14
14p		Me	H	H	3.54	310	2900	9
14q		Me	H	H	3.31	97	1200	12
14r		Me	H	H	3.01	2350	>10000	>4
14s		H	H	Me	3.31	490	>10000	>20

^a EC₅₀ values measured in a GTPγS assay using membranes of CHO cells expressing either S1PR₁ or S1PR₃; EC₅₀ values are the geometric mean of at least three independent measurements in duplicate.

^b Selectivity against S1PR₃ calculated as the ratio EC₅₀ S1PR₃/EC₅₀ S1PR₁.

to the alkylamino moiety was tolerated by S1PR₁ (**20f**), an additional dimethylamino group as in compound **20g** led to a significant potency loss. As in the benzene series, secondary amines showed a reduced activity when compared to the corresponding tertiary amine analogs (e.g. **20h** vs **20a**, **20i** vs **20e**). Removing the methyl

group in the 4 position (R₂) of the thiophene reduced the compound's affinity for both receptors (**20j–n**). Nevertheless, the thiophenes **20j** and **20m**, for instance, were still significantly more potent than their corresponding 4-aminomethyl benzenes **17i** and **17h**, respectively. Elongation of R₂ to an ethyl group improved the

compound's potency, in particular on S1PR₃ and the two ethyl derivatives **20o** and **20p** were the more potent dual S1PR_{1/3} agonists of this series. Compound **20o** was also less selective for S1PR₁ when compared to its 4-aminomethyl benzene analog **17l**. Finally, attaching a methyl group to position 3 (R₃) of thiophenes **20a**, **20c**, and **20e** gave analogs **20q**, **20r**, and **20s**, respectively, which were all less potent on S1PR₁ and S1PR₃. The affinity loss appears to be more pronounced for compounds bearing larger alkylaminomethyl groups (e.g. **20s**).

Overall, the SAR analysis indicated that all four series behave very similar in terms of selectivity against the S1P₃ receptor. On the other hand the 5-aminomethyl thiophene series appeared superior with respect to the affinity to the S1P₁ receptor. We observed in the 2-aminomethyl pyridine series that increasing the lipophilicity of the compounds gave a gain in potency (compare **11a** with **11c** and **11d** in Table 1) whereas in the other three series this gain was minimal (compare within subgroup **14a–e** (Table 2), or **17a–d** (Table 3), or **20a–e** (Table 4)).

2.3. Pharmacokinetics and pharmacodynamics

The metabolic stability (Table 5) of a few potent representatives from each subseries was studied using rat liver microsomes (RLM). There are clear differences in the apparent *in vitro* intrinsic clearance (CL_{int, app.}) not only between, but also within, the subseries. The pyridines appear to be less stable than the corresponding benzene and thiophene analogs. This is illustrated with the isobutyl derivative **11c**, which shows a 3–10 times higher CL_{int, app.} as compared to its benzene (**14e** and **17d**) and thiophene (**20e**) analogs. On the other hand, the size of the alkyl chain attached to the amino group influences the CL_{int, app.} as well. As illustrated with the four benzene compounds **14a**, **14b**, **14d** and **14e** the metabolic stability appears to improve with increasing size of the alkyl chain. While the dimethylamine derivative **14a** showed a high CL_{int, app.} of >1250 µL/min/mg, the corresponding isobutylmethyl amine **14e** appeared more stable with an apparent *in vitro* intrinsic clearance of 20 µL/min/mg. A similarly marked difference was observed between the dimethylamines **17l** and **20a**, and their corresponding isobutylmethylamine analogs **17d** and **20e**, respectively. It is well established that reliance on apparent *in vitro* intrinsic clearance (CL_{int, app.}) values for assessment of metabolic stability may be misleading due to nonspecific microsomal binding (f_{u, mic}), in particular for a series of lipophilic basic compounds like ours [72]. Table 5 demonstrates that CL_{int, app.} in RLM and f_{u, mic} decrease in parallel. This suggests that f_{u, mic} is a major determinant of “apparent” metabolic stability of those examples. Hence, the apparent gain in metabolic stability when looking at CL_{int, app.} values appears to be driven by the increase of microsomal binding rather than rendering the compounds worse substrates of the microsomal enzymes (compare **14a,b** with **14d**, and **17l** with **17d**). The increase in microsomal binding is known to follow lipophilicity as reflected in Table 5 (logD) [73,74]. Interestingly, when correcting the CL_{int, app.} for unbound fraction (CL_{int}), compounds **11c** and **14e** clearly stand out from the remainder of the S1PR₁ agonists exemplified suggesting that branched alkyl chains are less susceptible to metabolism compared to the straight chains.

In vivo efficacy of S1PR₁ agonists with an EC₅₀ below 10 nM on S1PR₁ was evaluated by measuring their ability to reduce the number of lymphocytes in blood. For a few compounds plasma exposure was measured at the same time points as LC was determined. Table 6 summarizes the pharmacodynamic profiles of the 2-alkylaminomethyl pyridine **11c**, the 3-alkylaminomethyl benzenes **14a,b,d,e**, the 4-alkylaminomethyl benzene **17l** and the 5-alkylaminomethyl thiophenes **20a** and **20e**, and the plasma concentrations of **11c**, **14e**, **20a** and **20e** after oral administration of

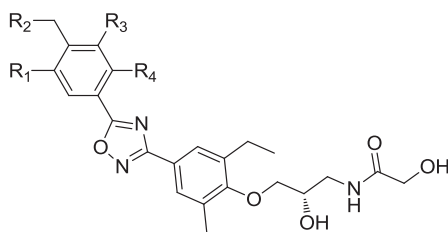
10 mg/kg to male Wistar rats. Blood lymphocyte count (LC) was measured shortly before and 3, 6, and 24 h after compound administration. Later sampling time points were added for compounds **14e** and **20e** to confirm complete recovery of the LC. Because of significant inter-individual variability and the circadian rhythm of the absolute number of circulating lymphocytes, a LC change of ±15% was considered to be within baseline. On the other hand, a LC reduction of ≥60% was interpreted as the maximal effect that is achieved under the experimental conditions chosen [47]. The duration of action (DA) was defined as the latest time point at which maximal LC reduction was observed.

We first looked at the plasma exposure of compounds **11c**, **14e**, **20a**, and **20e** to understand how *in vitro* clearance translated into *in vivo* clearance. We corrected the apparent intrinsic *in vitro* clearance of the four compounds for f_{u, mic} and scaled to total body weight (CL_{int, scaled}, Table 6). The two thiophenes **20a** and **20e** show similarly high scaled up CL_{int} values of 14600 and 25200 mL/min/kg, respectively. The lower oral plasma clearance of **20e** compared to **20a** (19 vs 275 mL/min/kg respectively) can be attributed to the significantly higher plasma protein binding of **20e** (Table 5) [72,75]. The high extent of plasma protein binding therefore protects **20e** from *in vivo* metabolism. Similarly, despite showing comparable values for CL_{int, scaled}, the pyridine **11c** and the benzene **14e** clearly show different oral plasma clearance (80 vs 8 mL/min/kg respectively). This can again be attributed to the significantly higher plasma protein binding of compound **14e**, which protects the compound from being metabolized *in vivo*.

With respect to efficacy, all compounds tested showed a rapid onset of action and the largest LC reduction was usually observed at 3 h after compound administration. LC reduction followed largely plasma exposure and usually returned to baseline 24 h after compound administration. Specifically, agonist **11c** produced maximal LC reduction (–80%) 3 h post dose and was of short duration only. Plasma concentrations of **11c** determined in the LC experiment reached a maximum of 385 ng/mL at 3 h after compound administration and were below 2 ng/mL at 24 h. The short duration of action reflected therefore the rapid decline in plasma exposure (oral plasma clearance CL/F = 80 mL/min/kg). When compared to pyridine **11c**, the 3-aminomethyl benzene analog **14e**, displayed a more sustained LC reduction for 24 h in line with its lower oral plasma clearance of 8 mL/min/kg. Interestingly, despite high exposure of **14e** at 3 and 6 h no maximal reduction of the circulating lymphocytes was observed. The reason for the submaximal efficacy remains unclear. For instance, neither in the GTPγS assay nor in receptor internalization assays did compound **14e** behave as a partial agonist (data not shown). Another explanation could be that the f_{u, p} of **14e** is much higher than 99.9% while, for instance, for the fully efficacious compound **20e** f_{u, p} could be close to 99.9%. In addition, differences in tissue distribution (e.g. plasma versus lymph) may account for the distinct efficacies [66,76]. A rather short DA (<6 h) was observed with analogs **14a,b,d** and **17l**. The two thiophenes **20a** and **20e** showed a clear difference in duration of action. While the number of circulating lymphocytes was back to baseline levels at 24 h after administration of dimethylamine **20a**, the LC was still maximally reduced at 24 h with low-clearance isobutylmethylamine **20e**. Calculating the free compound concentration available for receptor binding in plasma (free drug concentration = total plasma concentration × f_{u, p}) suggested that reaching concentrations of around EC₅₀ is sufficient to observe significant LC reduction.

Of the compounds discussed above, thiophene **20e** displayed the best *in vivo* efficacy along with high affinity and a more than 200-fold selectivity for S1PR₁ vs. S1PR₃ (EC₅₀ > 1000, 145, >1000, and 753 nM for S1PR₂, S1PR₃, S1PR₄ and S1PR₅, respectively). We therefore decided to characterize this compound in more detail.

Table 3
SAR of the 4-aminomethyl benzene series.



Compd	R ₁	R ₂	R ₃	R ₄	clogP	EC ₅₀ S1PR ₁ ^a [nM]	EC ₅₀ S1PR ₃ ^a [nM]	Selectivity ^b
17a	Me		H	H	2.23	7.1	3200	451
17b	Me		H	H	2.63	14	910	65
17c	Me		H	H	3.54	5.3	350	66
17d	Me		H	H	3.31	13	570	44
17e	Me		H	H	3.04	10	560	56
17f	Me		H	H	3.01	50	3100	62
17g	Me		H	H	3.04	270	>10000	>37
17h	H		H	H	1.88	160	>10000	>62
17i	H		H	H	1.62	2090	>10000	>4.8
17j	Me		Me	H	2.57	69	5500	>80
17k	H		H	Me	2.22	230	>10000	>43
17l	Et		H	H	2.64	1.3	480	369
17m	Et		H	H	3.05	1.0	100	100
17n	Et		H	H	3.46	1.0	210	210
17o	Et		H	H	3.43	3.5	4300	130

^a EC₅₀ values measured in a GTPγS assay using membranes of CHO cells expressing either S1PR₁ or S1PR₃; EC₅₀ values are the geometric mean of at least three independent measurements in duplicate.

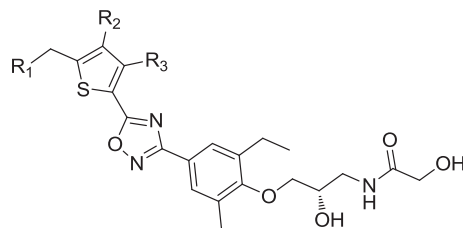
^b Selectivity against S1PR₃ calculated as the ratio EC₅₀ S1PR₃/EC₅₀ S1PR₁.

LC and plasma exposure were measured in a dose response experiment. The results listed in Table 7 demonstrate that plasma concentrations were dose proportional over the tested dose range and the whole time course. In addition, the reduction of the LC was clearly dose dependent. A single oral dose of 1 mg/kg reduced the LC by 46%, while a dose of 3 mg/kg induced already maximal LC reduction at 6 h. At 24 h, no effect on the number of circulating lymphocytes was observed anymore at the 1 mg/kg dose, while the 3 mg/kg dose still resulted in a LC reduction of 25%. As mentioned earlier, maximal LC reduction for at least 24 h was achieved with an oral dose of 10 mg/kg and the LC returned to baseline levels 96 h after dosing.

2.4. Brain penetration

In view of recent reports on CNS related autoimmune diseases, which suggest beneficial, direct effects of S1PR₁ agonists on cells of the central nervous system [36,38,39], we studied the potential of thiophene 20e to penetrate the brain in Wistar rats (Table 8). Based on parameters used to assess the CNS penetration potential of drug candidates (e.g. molecular weight, pKa, polar surface area, number of hydrogen bond donors) [77–80], compound 20e was predicted to have low permeability and thus a low probability to cross the blood brain barrier. As evident from the data in Table 8, thiophene 20e displayed a surprisingly good brain penetration, albeit brain

Table 4
SAR of the 5-aminomethyl thiophene series.



Compd	R ₁	R ₂	R ₃	clogP	EC ₅₀ S1PR ₁ ^a [nM]	EC ₅₀ S1PR ₃ ^a [nM]	Selectivity ^b
20a		Me	H	2.33	0.9	660	733
20b		Me	H	2.74	1.3	150	115
20c		Me	H	3.19	0.6	120	200
20d		Me	H	3.65	0.7	120	171
20e		Me	H	3.41	0.5	145	290
20f		Me	H	1.81	2.8	1700	607
20g		Me	H	2.03	155	>10000	>64
20h		Me	H	2.07	14	>10000	>714
20i		Me	H	3.15	20	1400	70
20j		H	H	1.72	189	>10000	>53
20k		H	H	2.12	293	>10000	>34
20l		H	H	2.49	203	>10000	>49
20m		H	H	1.99	5.4	>10000	>1852
20n		H	H	2.40	6.8	4600	676
20o		Et	H	2.75	0.3	45	150
20p		Et	H	3.61	0.5	20	40
20q		Me	Me	2.68	6.4	4400	687
20r		Me	Me	3.54	14	370	26
20s		Me	Me	3.76	55	2300	42

^a EC₅₀ values measured in a GTPγS assay using membranes of CHO cells expressing either S1PR₁ or S1PR₃; EC₅₀ values are the geometric mean of at least three independent measurements in duplicate.

^b Selectivity against S1PR₃ calculated as the ratio EC₅₀ S1PR₃/EC₅₀ S1PR₁.

Table 5
LogD, $f_{u,mic}$, $f_{u,p}$, apparent and corrected intrinsic clearance in rat liver microsomes.

Compd	$CL_{int, app}$ RLM ^a [μ L/min/mg]	logD ^b	$f_{u,mic}$ ^c	$f_{u,p}$ rat ^d	$CL_{int, RLM}$ ^e [μ L/min/mg]
11c	197	3.8	0.18*	0.004	1090
14a	>1250	2.8	0.26	0.029	>4800
14b	>1250	3.4	0.25*	0.012	>5000
14d	183	>4.1	0.025*	<0.001	7300
14e	20	>4.1	0.027	<0.001	740
17d	74	>4.1	0.001*	<0.001	74000
17l	1011	3.8	0.11*	0.005	9200
20a	1215	3.2	0.15	0.012	8100
20e	28	>4.1	0.002	<0.001	14000

* Recovery < 80%.

^a Apparent intrinsic clearance in the presence of rat liver microsomes at 1 μ M compound starting concentration.

^b Distribution coefficient between 1-octanol and phosphate buffer pH = 7.

^c Unbound fraction in microsomal incubations.

^d Unbound fraction in rat plasma.

^e Apparent intrinsic clearance corrected for unbound fraction, $CL_{int} = CL_{int,app}/f_{u,mic}$.

Table 6
Lymphocyte count, plasma concentrations, oral plasma clearance in male Wistar rats and scaled up *in vitro* CL_{int} .

Compd	LC reduction [%] ^a			Plasma concentration [ng/mL] ^b					CL/F ^d [mL/min/kg]	$CL_{int, scaled}$ ^e
	3 h	6 h	24 h	3 h	6 h	24 h	72 h	96 h		
11c	-80	-75	+1	385	176	<2	n.d.	n.d.	80	1970
14a	-44	-37	+21							
14b	-57	-58	+24							
14d	-60	-57	-6							
14e	-52	-53	-44	1377	1121	342	3.7	n.d.	8	1330
17l	-56	-61	+27							
20a	-64	-56	+5	106	31	<4			275	14600
20e	-69	-77	-70 ^c	722	541	92	n.d.	0.5	19	25200

n.d. = not determined.

^a Lymphocyte count reduction at indicated time point post compound administration as compared to vehicle treated group.

^b After oral administration of 10 mg/kg of aminomethyl aryl derivatives (n = 6).

^c +4% at 96 h.

^d Oral plasma clearance as estimated from the plasma concentration data.

^e *In vitro* clearance scaled up to full body weight according to $CL_{int} = \frac{CL_{int, app} \cdot SF}{f_{u,mic}}$, wherein the scaling factor (SF) is the product of 45 mg microsomal protein/g liver and 40 g liver/kg body weight = 1.8 including the change in units from μ L/min/mg ($CL_{int, app}$) to mL/min/kg ($CL_{int, scaled}$) [72].

exposure is clearly delayed as compared with plasma exposure. At 2 h after compound administration total brain concentration reached 522 ng/g, while total plasma concentration was somewhat higher with 783 ng/mL. Interestingly, 6 h after dosing brain concentration further increased to 1028 ng/g and exceeded that in plasma by a factor of 1.7. While the concentration in brain was still high at 24 h, the plasma concentration had dropped significantly. The observed shift between total plasma and brain concentration supports a rather slow passage of compound **20e** through the blood brain barrier. In a multiple dose experiment using 10 mg/kg, the brain concentration is expected to be >1000 ng/mL at steady state. Therefore, compound **20e** is potentially an interesting molecule to treat immune-mediated diseases, where activity in the brain is deemed beneficial or even required.

2.5. *In vitro* phototoxicity measurement

Representatives of the different amino-methyl aryl series were measured for their phototoxicity potential in the *in vitro* mouse 3T3 fibroblast (NRU) phototoxicity assay [60,61]. The obtained PIF values are summarized in Table 9. In contrast to aminopyridine **1** none of new compounds showed any sign of phototoxicity (PIF < 2.5). The only exception was the 5-aminomethyl thiophene **20e** for which the measured PIF value was 6. Further investigation showed that **20e** in particular displays some chemical instability and partially decomposes ($\leq 6\%$) to its corresponding aldehyde **19b** (Scheme 4 with $R_2 = Me$ and $R_3 = H$, EC_{50} S1PR₁ = 26 nM, S1PR₃

>10000 nM). This decomposition is more pronounced under UV conditions as indicated by LCMS analysis of aliquots exposed to the assay conditions (data not shown). The mechanism of the presumed air-oxidation is thought to involve a hydrogen abstraction by singlet oxygen followed by an electron transfer that generates the hydrolyzable iminium [81,82]. As aldehyde **19b** is clearly phototoxic (PIF = 31), it is not possible to accurately measure the PIF value of **20e**, but we can assume that the PIF value of **20e** is below 6. Close inspection of the chemical instability of other 5-aminomethyl thiophenes showed that they also partially decomposed but to a lesser extent (<1%).

Thus, we have reached our goal to find potent, selective and *in vivo* efficacious aminomethyl aryl S1PR₁ agonists that are devoid of phototoxic potential. However, as observed for the 5-aminomethyl thiophene **20e**, we now face chemical instability via air-oxidation to a phototoxic aldehyde which represents a strong obstacle to further develop this compound class.

3. Conclusions

With the aim to abolish the phototoxic potential of aminopyridine based S1PR₁ agonists such as **1**, we discovered a new class of potent, selective and *in vivo* active aminomethyl substituted pyridine derivatives. Low nanomolar affinity of compound **11c** illustrated that the S1P₁ receptor can accommodate the basic aminomethyl moiety. However, these aminomethyl pyridine based S1PR₁ agonists suffered from metabolic instability which translated

Table 7

Lymphocyte count and plasma concentrations after p.o administration of 20e to male Wistar rats.^a

Dose [mg/kg]	LC reduction [%]				Plasma concentration [ng/mL]				
	3 h	6 h	24 h	96 h	3 h	6 h	24 h	72 h	96 h
1	-33	-46	+4		67	49	5.2	BLQ	
3	-59	-70	-25		210	170	25	BLQ	
10	-69	-76	-70	+4	722	540	92	n.d.	0.5

^a n = 6; n.d.: not determined; BLQ: below limit of quantification.

into low exposure and a short duration of action in our *in vivo* model. Further structural modifications replacing the pyridine ring by a benzene or a thiophene ring led to new series of potent S1PR₁ agonists with higher *in vivo* exposure and *in vivo* efficacy. The 5-isobutylmethyl aminomethyl thiophene **20e**, a representative of the most interesting series, displayed low nanomolar affinity for S1PR₁ and a more than 200-fold selectivity vs. the S1PR₃. *In vivo* **20e** showed a dose dependent reduction of the number of circulating lymphocytes. At a dose of 10 mg/kg, maximal LC reduction was observed for 24 h and the effect was fully reversible within 96 h. Interestingly, the basic S1PR₁ agonist **20e** penetrated well into brain, making **20e** an interesting candidate for immune-mediated diseases for which activity in the brain is beneficial or even required. In addition, all representatives showed a PIF value far below the one measured for the original aminopyridine series. However, as the alkyl-aminomethyl thiophenes suffer from slow oxidation in the air, we decided to explore other chemical modifications to abolish the phototoxic potential observed in the aminopyridine-based S1PR₁ agonist series. The results of these investigations will be discussed in a follow-up publication [83].

4. Experimental section

4.1. Chemistry

All reagents and solvents were used as purchased from commercial sources (Sigma–Aldrich Switzerland, Lancaster Synthesis GmbH, Germany, Acros Organics USA). Moisture sensitive reactions were carried out under an argon atmosphere. Progress of the reactions was followed either by thin-layer chromatography (TLC) analysis (Merck, 0.2 mm silica gel 60 F₂₅₄ on glass plates) or by LC-MS. LC-MS parameters: Finnigan MSQ™ plus or MSQ™ surveyor (Dionex, Switzerland), with HP 1100 Binary Pump and DAD (Agilent, Switzerland), column: Zorbax SB-AQ, 5 μm, 120 Å, 4.6 × 50 mm (Agilent), gradient: 5–95% acetonitrile in water containing 0.04% of trifluoroacetic acid, within 1 min, flow: 4.5 mL/min; t_R is given in min. LC-MS marked with * refers to LC run on Zorbax SB-AQ, 1.8 μm, 4.6 × 20 mm. LC-MS marked with ** refers to LC run on Waters X-Bridge C18, 5 μm, 4.6 × 50 mm under basic conditions, i.e. eluting with a gradient of MeCN in water containing 13 mM of ammonium hydroxide.

According to the LC-MS analyses, final compounds showed a purity >95% (UV at 230 nm and 214 nm) except for compounds **14a**, **14k**, **17i**, **20k** and **20p** with purities of 90–93%. Purity and identity was further confirmed by LC-HRMS and NMR

Table 8

Total brain and plasma concentrations of 20e after single oral dose of 10 mg/kg in Wistar rats.

Time (h)	Total plasma concentration ^a [ng/mL]	Total brain concentration ^a [ng/g]	Brain/plasma ratio
2	783 ± 149	522 ± 212	0.64 ± 0.15
6	622 ± 86	1028 ± 6	1.69 ± 0.24
24	66.5 ± 15.6	776 ± 230	11.49 ± 0.75

^a Values are the mean of n = 2 animals.

Table 9

Photo-irritancy factor (PIF) values of some representatives of the four alkyl-aminomethyl substituted aryl series.

Compd	PIF value ^a	Comment
1	>200	phototoxic
5	1	clean
11a	1	clean
11c	1	clean
14e	1	clean
17a	1	clean
17i	1	clean
20a	1	clean
20c	1	clean
20e	≤6	partial oxidation into 19b
19b	31	phototoxic

^a Values measured in the *in vitro* mouse 3T3 fibroblast neutral red uptake (NRU) phototoxicity assay (see Supplementary Material for details); mean of n = 2.

spectroscopy. **LC-HRMS**: Analytical pump = Waters Acquity Binary, Solvent Manager, MS: SYNAPT G2 MS, source temperature: 150 °C, desolvation temperature: 400 °C, desolvation gas flow: 400 L/hr; cone gas flow: 10 L/hr, extraction cone: 4 RF; lens: 0.1 V; sampling cone: 30; capillary: 1.5 kV; high resolution mode; gain: 1.0, MS function: 0.2 s per scan, 120–1000 amu in full scan, centroid mode. Lock spray: Leucine enkephalin 2 ng/mL (556.2771 Da) scan time 0.2 s with interval of 10 s and average of 5 scans; DAD: Acquity UPLC PDA Detector. Column: Acquity UPLC BEH C18 1.7 μm 2.1 × 50 mm from Waters, thermostated in the Acquity UPLC Column Manager at 60 °C. Eluents: water +0.05% formic acid; B: acetonitrile +0.05% formic acid. Gradient: 2–98% B over 3.0 min. Flow: 0.6 mL/min. Detection: UV 214 nm and MS, t_R is given in min. **NMR spectroscopy**: Bruker Avance II, 400 MHz UltraShield™, 400 MHz (¹H), 100 MHz (¹³C); or Bruker Avance III HD, Ascend 500 MHz (¹H), 125 MHz (¹³C) magnet equipped with DCH cryoprobe, chemical shifts are reported in parts per million (ppm) relative to tetramethylsilane (TMS), and multiplicities are given as s (singlet), d (doublet), t (triplet), q (quartet), quint (quintuplet), h (hexet), hept (heptuplet) or m (multiplet), br = broad, coupling constants are given in Hz. Several compounds have been prepared on a 15–50 mmol scale. For those compounds ¹H NMR spectra were acquired using non-deuterated 10 mM DMSO stock solution submitted for biological testing [84]. The solvent and water signals were suppressed by irradiation at 2.54 and 3.54 ppm, respectively. As a consequence, signal integrals close to those frequencies are not always accurate or visible. Compounds were purified by either flash **column chromatography** on silica gel 60 (Fluka Sigma–Aldrich, Switzerland), or by **prep. HPLC** (Waters XBridge™ Prep C18, 5 μm, OBD, 19 × 50 mm, or Waters X-terra™ RP18, 19 × 50 mm, 5 μm, gradient of acetonitrile in water containing 0.4% of formic acid, flow 75 mL/min), or by **MPLC** (Labomatic MD-80-100 pump, Linear UVIS-201 detector, column: 350 × 18 mm, Labogel-RP-18-5s-100, gradient: 10% methanol in water to 100% methanol).

4.1.1. 2-(Hydroxymethyl)-6-methylisonicotinic acid methyl ester (8)

A suspension of 2-methylpyridine-4-carboxylic acid **7** (5.0 g, 36.5 mmol) in methanol (500 mL) was treated with concentrated

sulfuric acid (2.5 mL). The white suspension is refluxed for 24 h to give a clear solution of the corresponding ester. A solution of ammonium persulfate (16.6 g, 72.9 mmol) in water (40 mL) was then added and the reaction mixture was stirred at reflux for 4 h. Another 20 mL of ammonium persulfate aq. solution (8.3 g, 36.5 mmol) were added. After another 6 h at reflux, the reaction mixture was concentrated and partitioned between EA (300 mL) and NaHCO₃ (6 × 100 mL). The organic phase was dried over MgSO₄, filtered and evaporated to give a residue which was purified by prep. HPLC (XBridge Prep C18) to afford 2-hydroxymethyl-6-methyl-isonicotinic acid methyl ester as a white crystalline solid (4.07 g, 62%); LC-MS^{**}: t_R = 0.61 min, [M+1]⁺ = 182.25; ¹H NMR (D₆-DMSO): δ 7.74 (s, 1 H), 7.57 (s, 1 H), 5.54 (t, J = 5.8 Hz, 1 H), 4.59 (d, J = 5.8 Hz, 2 H), 3.90 (s, 3 H), 2.53 (s, 3 H).

4.1.2. 2-((Isobutyl(methyl)amino)methyl)-6-methylisonicotinic acid (9c)

a) To a solution of 2-(hydroxymethyl)-6-methylisonicotinic acid methyl ester (2.83 g, 15.6 mmol) and DIPEA (8.0 mL, 46.9 mmol) in DCM (250 mL) was added methanesulfonyl chloride (1.46 mL, 18.7 mmol). The reaction mixture was stirred at rt for 1 h and was then washed with 1N Na₂CO₃ (50 mL), followed by 1N HCl (50 mL), water (25 mL) and brine (25 mL). The organic phase was dried over MgSO₄, filtered and evaporated to give the crude 2-methyl-6-(((methylsulfonyl)oxy)methyl)isonicotinic acid methyl ester (4.57 g crude containing about 15% of methyl 2-(chloromethyl)-6-methylisonicotinate as side product, 96%) which was used without purification. LC-MS^{**}: t_R = 0.73 min, [M+1]⁺ = 259.84.

b) To a solution of 2-methyl-6-(((methylsulfonyl)oxy)methyl)isonicotinic acid methyl ester (557 mg, 2.15 mmol) in acetonitrile (3 mL) was added a *N*-methylisobutylamine (562 mg, 6.44 mmol). The reaction mixture was stirred at 45 °C for 3 h. The reaction mixture was concentrated. Crude methyl 2-((isobutyl(methyl)amino)-methyl)-6-methylisonicotinate (482 mg) was then dissolved in 10 mL MeOH/THF (4:1), treated with 2N LiOH (3.0 mL) and stirred for 1 h to hydrolyze the ester to the corresponding acid. The reaction mixture was then concentrated to afford the title compound **9c** as a beige wax (490 mg crude, 96%); LC-MS^{**}: t_R = 0.50 min, [M+1]⁺ = 237.20. ¹H NMR (CDCl₃): δ 7.55 (s, 1 H), 7.34 (s, 1 H), 3.40 (s, 2 H), 2.19 (s, 3 H), 2.08–2.01 (m, 2 H), 1.98 (s, 3H), 1.68–1.56 (m, 1 H), 0.69 (d, J = 6.4 Hz, 6 H).

4.1.3. (S)-N-(3-(2-ethyl-4-(5-(2-((isobutyl(methyl)amino)methyl)-6-methylpyridin-4-yl)-1,2,4-oxadiazol-3-yl)-6-methylphenoxy)-2-hydroxypropyl)-2-hydroxyacetamide (11c)

To a solution of 2-((isobutyl(methyl)amino)methyl)-6-methylisonicotinic acid **9c** (385 mg, 1.63 mmol) and (S)-N-(3-(2-ethyl-4-(*N*-hydroxycarbamimidoyl)-6-methylphenoxy)-2-hydroxypropyl)-2-hydroxyacetamide **10** [59] (562 mg, 1.73 mmol) in DMF (3.0 mL), HOBt (264 mg, 1.96 mmol) and EDC (375 mg, 1.96 mmol) were added. The reaction mixture was stirred at rt overnight and was then diluted with EA (150 mL), washed with sat. NaHCO₃ (25 mL) followed by brine (25 mL). The organic phase was dried over MgSO₄, filtered and evaporated to give an orange residue (886 mg) which was dissolved in dioxane (120 mL) and heated at 100 °C for 18 h. The reaction mixture was concentrated and the residue was purified by prep. HPLC (Waters X-Bridge C18, gradient of acetonitrile in water containing 0.5% NH₄OH) to give **11c** (415 mg, 48%) as a beige solid; LC-MS^{**}: t_R = 0.97 min, [M+1]⁺ = 526.12; HRMS (ESI⁺) *m/z* calculated for C₂₈H₃₉N₅O₅ [M+1]⁺ 526.3029, found 526.3033; ¹H NMR (D₆-DMSO): δ 7.97 (s, 1 H), 7.85 (s, 1 H), 7.79 (s, 2 H), 7.72 (t, J = 5.7 Hz, 1 H), 5.57 (t, J = 5.7 Hz, 1 H), 5.33 (d, J = 5.1 Hz, 1 H), 4.01–3.92 (m, 1 H), 3.84 (d, J = 5.7 Hz, 2 H), 3.77 (dd, J₁ = 9.5 Hz, J₂ = 4.6 Hz, 1 H), 3.72 (dd, J₁ = 9.5 Hz, J₂ = 6.1 Hz, 1 H), 3.67 (s, 2 H), 3.48–3.39 (m, 1 H), 3.30–3.20 (m, 1 H), 2.73 (q,

J = 7.5 Hz, 2 H), 2.60 (s, 3 H), 2.35 (s, 3 H), 2.23 (s, 3 H), 2.16 (d, J = 7.3 Hz, 2 H), 1.89–1.78 (m, 1 H), 1.22 (t, J = 7.5 Hz, 3 H), 0.91 (d, J = 6.5 Hz, 6 H); ¹³C NMR (D₆-DMSO): δ 174.5, 172.4, 168.7, 161.7, 159.5, 158.4, 138.2, 132.4, 131.4, 128.2, 126.4, 121.8, 119.1, 117.2, 75.7, 69.1, 66.0, 63.9, 61.9, 43.1, 41.9, 26.1, 24.4, 22.6, 21.1, 16.6, 15.2.

4.1.4. 3-Formyl-5-methyl-benzoic acid (12a) [68].

a) A solution of 2,5-dimethyl benzoic acid (42.0 g, 282 mmol), 2,2'-azo-bis(2-methylpropionitrile) (4.73 g, 28.2 mmol) and *N*-bromo-succinimide (52.7 g, 296 mmol) in DCM (1.1 L) was refluxed for 18 h. The mixture was extracted with 1 N aq. NaOH and water. The combined aqueous extracts were acidified by adding 1 N aq. HCl and extracted with twice EA. The combined org. extracts were washed with water, dried over Na₂SO₄, filtered and concentrated. The crude product was crystallized from hot EtOH (25 mL) by adding cold water (50 mL). The mixture was cooled to rt, the crystallized material was collected and dried to give 3-bromomethyl-5-methyl-benzoic acid (32.0 g) as a white solid; LC-MS^{*}: t_R = 0.95 min, [M+1]⁺ = not detectable.

b) To a solution of 3-bromomethyl-5-methyl-benzoic acid (3.90 g, 17 mmol) in water (30 mL) and MeCN (30 mL), Cu(NO₃)₂ hemipentahydrate (12.77 g, 68 mmol) followed by water (50 mL) was added. The turquoise mixture was refluxed for 2 h before it was concentrated to about half of the original volume. The dark green solution was extracted three times with EA (150 mL). The org. extracts were washed twice with water (2 × 50 mL), combined, dried over Na₂SO₄, filtered and concentrated. The white residue was separated by prep. HPLC (XBridge Prep C18) to give 3-hydroxymethyl-5-methyl-benzoic acid (897 mg) as a white solid, LC-MS: t_R = 0.64 min ([M+1]⁺ = not detected), along with the title compound (160 mg) as a white solid. To a solution of the above 3-hydroxymethyl-5-methyl-benzoic acid (947 mg, 5.70 mmol) in MeCN (40 mL), MnO₂ (1.49 g, 17.1 mmol) was added and the resulting mixture was stirred at 80 °C for 16 h before another portion of MnO₂ (1.21 g, 13.9 mmol) and acetonitrile (40 mL) were added and stirring was continued at 80 °C for 4 h. The mixture was filtered over a glass fibre filter, the colourless filtrate was concentrated and purified by prep. HPLC (as above) to give the title compound **12a** (504 mg) as a white solid; LC-MS: t_R = 0.64 min, [M+1]⁺ = not detectable; ¹H NMR (D₆-DMSO): δ 13.29 (s, 1 H), 10.06 (s, 1 H), 8.26 (s, 1 H), 8.07 (s, 1 H), 7.96 (s, 1 H), 2.47 (s, 3 H).

4.1.5. (S)-N-(3-(2-ethyl-4-(5-(3-((isobutyl(methyl)amino)methyl)-5-methylphenyl)-1,2,4-oxadiazol-3-yl)-6-methylphenoxy)-2-hydroxypropyl)-2-hydroxyacetamide (14e)

a) A solution of 3-formyl-5-methyl-benzoic acid **12a** (340 mg, 2.1 mmol), HOBt (336 mg, 2.5 mmol) and EDC (437 mg, 2.3 mmol) in DMF (40 mL) was stirred at rt for 30 min before adding *N*-((S)-3-[2-ethyl-4-(*N*-hydroxycarbamimidoyl)-6-methyl-phenoxy]-2-hydroxy-propyl)-2-hydroxy-acetamide **10** [59] (674 mg, 2.1 mmol). The mixture was stirred at rt for 18 h and was then diluted with EA (50 mL), washed with sat. NaHCO₃ (25 mL), followed by brine (25 mL). The organic phase was dried over MgSO₄, filtered and concentrated. The orange residue was dissolved in dioxane (120 mL) and heated at 100 °C for 2 h. The reaction mixture was then evaporated and the crude compound was purified by CC (eluent DCM/MeOH 9:1) to afford (S)-N-(3-(2-ethyl-4-(5-(3-formyl-5-methylphenyl)-1,2,4-oxadiazol-3-yl)-6-methyl-phenoxy)-2-hydroxypropyl)-2-hydroxyacetamide **13a** (407 mg, 43%); LC-MS: t_R = 0.85 min, [M+1]⁺ = 454.11; ¹H NMR (D₆-DMSO): δ 10.15 (s, 1 H), 8.50 (s, 1 H), 8.34 (s, 1 H), 8.06 (s, 1 H), 7.82 (s, 2 H), 7.71 (t, J = 5.0 Hz, 1 H), 5.56 (t, J = 5.5 Hz, 1 H), 5.32 (d, J = 4.6 Hz, 1 H), 4.01–3.93 (m, 1 H), 3.84 (d, J = 4.7 Hz, 2 H), 3.81–3.71 (m, 2 H), 3.39–3.48 (m, 1 H), 3.30–3.19 (m, 1 H), 2.74 (q, J = 7.3 Hz, 2 H), 2.55 (s, 3 H), 2.36 (s, 3 H), 1.23 (t, J = 7.4 Hz, 3 H).

b) *N*-methylisobutylamine (78 μ L, 0.65 mmol) was added to a suspension of (*S*)-*N*-(3-(2-ethyl-4-(5-(3-formylphenyl)-1,2,4-oxadiazol-3-yl)-6-methylphenoxy)-2-hydroxypropyl)-2-hydroxyacetamide **13a** (103 mg, 0.24 mmol) in DCM (10 mL) and NMP (2.0 mL). The reaction mixture was stirred at rt for 1 h and was then cooled to 0 °C and NaBH(OAc)₃ (250 mg, 1.18 mmol) was added followed by acetic acid (0.4 mL). The reaction mixture was warmed to rt and stirred for 18 h. The reaction was then quenched with MeOH (3 mL) and concentrated to give an orange wax which was purified by prep-HPLC (XBridge Prep C18, gradient of acetonitrile in water containing 0.5% NH₄OH) to afford the title compound **14e** (55.4 mg, 48%); LC-MS*: $t_R = 0.58$ min, $[M+1]^+ = 525.38$; HRMS (ESI+) m/z calculated for C₂₉H₄₀N₄O₅ $[M+1]^+ 525.3077$, found 525.3080; ¹H NMR (D₆-DMSO): δ 7.94 (s, 1 H), 7.90 (s, 1 H), 7.79 (s, 2 H), 7.69 (t, $J = 5.3$ Hz, 1 H), 7.47 (s, 1 H), 5.55 (t, $J = 5.7$ Hz, 1 H), 5.31 (d, $J = 5.2$ Hz, 1 H), 3.96–3.93 (m, 1 H), 3.84 (d, $J = 5.7$ Hz, 2 H), 3.81–3.70 (m, 2 H), 3.54 (s, 2 H), 3.48–3.40 (m, 1 H), 3.29–3.21 (m, 1 H), 2.73 (q, $J = 7.8$ Hz, 2 H), 2.44 (s, 3 H), 2.35 (s, 3 H), 2.15 (s, 3 H), 2.12 (d, $J = 7.3$ Hz, 2 H), 1.88–1.77 (m, 1 H), 1.23 (t, $J = 7.5$ Hz, 3 H), 0.89 (d, $J = 6.5$ Hz, 6 H); ¹³C NMR (CDCl₃): δ 176.0, 172.6, 168.6, 157.6, 141.0, 138.9, 137.5, 134.1, 131.5, 128.4, 127.3, 126.7, 125.7, 124.0, 123.1, 74.0, 70.3, 66.2, 62.2, 42.7, 42.2, 26.2, 22.9, 21.3, 20.9, 16.5, 14.8.

4.1.6. 3-Ethyl-4-formyl-benzoic acid (**15e**) [68].

a) 4-Formyl-3-hydroxy-benzoic acid (1.5 g, 9.0 mmol) and pyridine (2.9 mL, 36.1 mmol) were dissolved in DCM (50 mL). The solution was cooled to 0 °C before adding triflic anhydride (3.1 mL, 19 mmol) and was then stirred for 1 h. The reaction mixture was quenched with 1 mL NH₄OH, evaporated and the crude compound was purified by prep. HPLC (XBridge Prep C18) to give 4-formyl-3-(((trifluoromethyl)sulfonyl)oxy)benzoic acid (413 mg, 15%). LC-MS*: $t_R = 0.52$ min, $[M+1]^+ =$ not detectable; ¹H NMR (D₈-THF): δ 9.03 (s, 1 H), 8.40 (s, 1 H), 6.40 (d, $J = 8.0$ Hz, 1 H), 6.30 (d, $J = 8.0$ Hz, 1 H), 6.24 (s, 1 H).

b) To a solution of 4-formyl-3-(((trifluoromethyl)sulfonyl)oxy)benzoic acid (200 mg, 0.67 mmol) in dioxane (5 mL) was added Pd(dppf)Cl₂ (4.5 mg, 0.01 eq.) under nitrogen atmosphere. Diethyl zinc (15wt % in toluene, 0.9 mL, 1.0 mmol) was then added dropwise and the reaction mixture was stirred at 75 °C for 1 h. After evaporation, the crude compound was purified by prep. HPLC (XBridge Prep C18) to give the title compound (66 mg, 55%). LC-MS*: $t_R = 0.62$ min, $[M+1]^+ =$ not detectable; ¹H NMR (D₆-DMSO): δ 13.36 (s br, 1 H), 10.34 (s, 1 H), 7.94 (s, 2 H), 7.93 (s, 1 H), 3.10 (q, $J = 7.5$ Hz, 2 H), 1.21 (t, $J = 7.5$ Hz, 3 H).

4.1.7. (*S*)-*N*-(3-(4-(5-(4-((dimethylamino)methyl)-3-ethylphenyl)-1,2,4-oxadiazol-3-yl)-2-ethyl-6-methylphenoxy)-2-hydroxypropyl)-2-hydroxyacetamide (**17l**)

The title compound was prepared in analogy to compound **14e** starting from 3-ethyl 4-formyl benzoic acid **15e** and using 2N dimethylamine in THF and NaBH(OAc)₃ for the reductive amination (48 mg); LC-MS*: $t_R = 0.53$ min, $[M+1]^+ = 497.80$; HRMS (ESI+) m/z calculated for C₂₇H₃₆N₄O₅ $[M+1]^+ 497.2764$, found 497.2758; ¹H NMR (CDCl₃): δ 8.06 (s, 1 H), 8.02 (dd, $J_1 = 1.6$ Hz, $J_2 = 7.9$ Hz, 1 H), 7.88 (s, 1 H), 7.86 (s, 1 H), 7.54 (d, $J = 8.0$ Hz, 1 H), 7.08 (t, $J = 5.8$ Hz, 1 H), 4.24–4.16 (m, 3 H), 3.89 (dd, $J_1 = 4.7$ Hz, $J_2 = 9.6$ Hz, 1 H), 3.84 (dd, $J_1 = 6.2$ Hz, $J_2 = 9.5$ Hz, 1 H), 3.81–3.75 (m, 1 H), 3.56–3.46 (m, 3 H), 2.85 (q, $J = 7.5$ Hz, 2 H), 2.74 (q, $J = 7.5$ Hz, 2 H), 2.38 (s, 3 H), 2.31 (s, 6 H), 1.32 (t, $J = 7.5$ Hz, 6 H); ¹³C NMR (CDCl₃): δ 175.8, 172.8, 168.6, 157.0, 144.2, 141.8, 137.5, 131.5, 130.5, 128.4, 128.2, 126.7, 125.4, 123.1, 123.0, 74.0, 70.3, 62.2, 61.1, 45.6, 42.2, 25.3, 22.9, 16.5, 15.0, 14.8.

4.1.8. 5-Formyl-4-methyl-thiophene-2-carboxylic acid (**18b**)

The title compound is prepared from commercially available 3-

methyl-2-thiophencarboxylic acid according to the procedures described in the literature [46,70]; LC-MS: $t_R = 0.70$ min, $[M+1]^+ =$ not detectable, ¹H NMR (D₆-DMSO): δ 13.67 (s br, 1 H), 10.09 (s, 1 H), 7.67 (s, 1 H), 2.57 (s, 3 H).

4.1.9. (*S*)-*N*-(3-(2-ethyl-4-(5-(5-((isobutyl(methyl)amino)methyl)-4-methylthiophen-2-yl)-1,2,4-oxadiazol-3-yl)-6-methylphenoxy)-2-hydroxypropyl)-2-hydroxy-acetamide (**20e**)

The title compound was prepared in analogy to compound **14e** starting from **18b** and using *N*-isobutylmethylamine for the reductive amination (82 mg); LC-MS: $t_R = 0.77$ min; $[M+1]^+ = 531.32$; HRMS (ESI+) m/z calculated for C₂₇H₃₈N₄O₅S $[M+1]^+ 531.2681$, found 531.2645; ¹H NMR (D₆-DMSO): δ 7.82 (s, 1 H), 7.73 (s, 2 H), 7.69 (t, $J = 5.8$ Hz, 1 H), 5.55 (t, $J = 5.7$ Hz, 1 H), 5.30 (d, $J = 5.2$ Hz, 1 H), 4.00–3.91 (m, 1 H), 3.84 (d, $J = 5.7$ Hz, 2 H), 3.77 (dd, $J_1 = 9.7$ Hz, $J_2 = 4.5$ Hz, 1 H), 3.72 (dd, $J_1 = 9.7$ Hz, $J_2 = 6.1$ Hz, 1 H), 3.67 (s, 2 H), 3.48–3.39 (m, 1 H), 3.29–3.20 (m, 1 H), 2.72 (q, $J = 7.5$ Hz, 2 H), 2.34 (s, 3 H), 2.23 (s, 6 H), 2.21 (d, $J = 7.4$ Hz, 2 H), 1.87–1.75 (m, 1 H), 1.22 (t, $J = 7.5$ Hz, 3 H), 0.91 (d, $J = 6.6$ Hz, 6 H). ¹³C NMR (CD₃OD): δ 174.1, 171.6, 168.3, 157.8, 146.4, 137.8, 135.6, 134.5, 131.8, 127.8, 126.1, 122.3, 122.2, 74.6, 69.1, 65.9, 61.2, 54.9, 41.8, 41.6, 26.2, 22.5, 19.8, 15.3, 14.0, 12.5. Despite purification by prep. HPLC the product always contained a few % of aldehyde **19b** according to the LCMS and NMR analysis.

In vitro 3T3 Neutral Red Uptake (NRU) Phototoxicity Test.

[60,61] The 3T3 NRU phototoxicity assay utilizes normal Balb/c 3T3 mouse fibroblasts to measure the concentration-dependent reduction in neutral red uptake by the cells one day after treatment with the chemical either in the presence or in the absence of a non-cytotoxic dose of UVA radiation. Balb/c 3T3 cells (clone 31, ECACC) were cultured overnight in duplicate 96-well microtiter plates at a density of 1×10^4 cells/100 μ L in Dulbecco's modified Eagle's medium (DMEM) containing 10% new born calf serum (NBCS, PAA B15-102), 4 mM L-glutamine, 100 U/ml penicillin and 100 μ g/mL streptomycin. The next day the cells were washed with phosphate buffered saline containing CaCl₂ and MgCl₂ (PBS⁺⁺). 3T3 fibroblasts were exposed to eight different concentrations of chemical, ranging from 0.05 to 100 μ M, with a pre-incubation time of 1 h (at 37 °C, 5% CO₂). One of the duplicate plates was exposed to 4 J/cm² UVA (1.7 mW/cm²) for 40 min while the other plate was kept in the dark. By using the UV-sun simulator UVACUBE 400 equipped with a SOL500 lamp and an H1-Filter (H1 Filter and frame: Cat. Number 4730, Dr. Hönle UV Technology) a UV-spectrum almost devoid of UVB is obtained. After UV exposure, PBS⁺⁺ was replaced with culture medium and cell viability was assessed after 24 h. The NRU by cells was measured at 540 nm and the absorption of wells exposed to the test chemical in the presence of UVA exposure (+UVA) was compared to their NRU in the absence of UVA exposure (-UVA). Dose-response curves were established for each experiment. EC₅₀ (+UVA) and EC₅₀ (-UVA) values, i.e. the effective concentration inhibiting cell viability by 50% of untreated controls in the presence and absence of UVA exposure, were calculated by using Phototox software version 2.0 [61]. The software was obtained at http://www.oecd.org/document/55/0,3343,en_2649_34377_2349687_1_1_1_1,00.html. Chlorpromazine (Sigma–Aldrich C0982-5G) served as the positive control. A PIF was calculated according to the formula $PIF = EC_{50}(-UVA)/EC_{50}(+UVA)$. PIF values > 2.5 were considered to be predictive for phototoxic potential.

In vitro potency assessment using GTP γ S binding assays.

GTP γ S binding assays were performed in 96 well polypropylene microtiter plates in a final volume of 200 μ L. Membrane preparations of CHO cells expressing recombinant human S1P₁ or S1P₃ receptors were used. Assay conditions were 20 mM Hepes, pH 7.4, 100 mM NaCl, 5 mM MgCl₂, 0.1% fatty acid free BSA, 1 or 3 μ M GDP

(for S1P₁ or S1P₃, respectively), 2.5% DMSO and 50 pM ³⁵S-GTPγS. Test compounds were dissolved, diluted and pre-incubated with the membranes, in the absence of ³⁵S-GTPγS, in 150 μL assay buffer at rt for 30 min. After addition of 50 μL of ³⁵S-GTPγS in assay buffer, the reaction mixture was incubated for 1 h at rt. The assay was terminated by filtration of the reaction mixture through a Multi-screen GF/C plate, pre-wetted with ice-cold 50 mM Hepes pH 7.4, 100 mM NaCl, 5 mM MgCl₂, 0.4% fatty acid free BSA, using a Cell Harvester. The filterplates were then washed with ice-cold 10 mM Na₂HPO₄/NaH₂PO₄ (70%/30%, w/w) containing 0.1% fatty acid free BSA. Then the plates were dried, sealed, 25 μL MicroScint20 was added, and membrane-bound ³⁵S-GTPγS was determined on the TopCount. Specific ³⁵S-GTPγS binding was determined by subtracting non-specific binding (the signal obtained in the absence of agonist) from maximal binding (the signal obtained with 10 μM S1P). The EC₅₀ of a test compound is the concentration of a compound inducing 50% of specific binding. Data (EC₅₀) are given as geometric means. Our assay sensitivity allows the accurate measurement of EC₅₀ as low as 0.1 nM.

The *In Vivo* Efficacy of the target compounds was assessed by measuring the circulating lymphocytes after oral administration of 1–10 mg/kg of a target compound to male Wistar rats. Male Wistar rats (RccHan:WIST) were obtained from Harlan Laboratories (Venray, the Netherlands). This study was conducted in accordance with Swiss Animal Protection Laws and with local guidelines (Basel-Landschaft Cantonal Veterinary Office). The animals were housed in climate-controlled conditions with a 12 h-light/dark cycle, and had free access to normal rat chow and drinking water. Blood was collected under isoflurane anaesthesia by sublingual vein puncture shortly before and 3, 6 and 24 h after drug administration. For several compounds later sampling time points were added to confirm complete recovery of the LC. Full blood was subjected to hematology using Beckman Coulter AcT 5diff CP (Beckman Coulter International SA, Nyon, Switzerland). The effect on lymphocyte count (%LC) was calculated for each animal as the difference between LC at a given time point and the pre-dose value (= 100%). All data are presented as mean of 6 animals. A lymphocyte count (LC) reduction of ≥ -60% was interpreted as the maximal effect that is achieved under this experimental conditions. For formulation, the compounds were dissolved in DMSO. This solution was added to a stirred solution of succinylated gelatine (7.5%) in water. The resulting milky suspension containing a final concentration of 5% of DMSO was administered to the animals by gavage.

***In vitro* CL_{int} determinations.** Intrinsic metabolic clearance (CL_{int}) was determined by substrate depletion experiments, with a default starting concentration of 1 μM in the presence of 0.5 mg/mL rat liver microsomes (RLM) in 100 mM sodium phosphate buffer, at pH 7.4. Incubations were initiated by the addition of an NADPH regenerating system. All incubations were conducted by shaking reaction mixtures under air, at 37 °C. Aliquots (0.1 ml) were removed at 0, 2.5, 5, 10 and 15 min and 0.1 mL of ice-cold methanol was added. After protein precipitation, by centrifugation, the remaining concentrations were analyzed by liquid chromatography coupled to mass spectrometry (LC-MS/MS), CL_{int} was calculated from the concentration remaining versus time, fitted to a first order decay constant versus time [85].

Free fraction in plasma microsomal incubations. The free fraction in rat plasma and in rat liver microsomes were determined by equilibrium analysis using a Pierce rapid equilibrium dialysis (RED) device (Thermo Fisher Scientific, Lausanne, Switzerland) by incubating on a shaker at 37 °C for 6 h. The donor compartment was either rat plasma (pH 7.2–7.6) or 1 mg/mL liver microsomes in phosphate buffer (pH 7.4). Donor and receiver (containing phosphate buffer, pH 7.4) were analyzed by LC-MS/MS and the free fraction and recovery were calculated.

Pharmacokinetics in the Rat. Blood samples were obtained from the above *in vivo* efficacy experiments in vials containing EDTA as anticoagulant and plasma was prepared by centrifugation at 3000 g for 10 min at 4 °C. Plasma samples were analyzed using liquid chromatography coupled to mass spectrometry (LC-MS/MS) after protein precipitation.

In vivo intrinsic clearances were derived from measured plasma concentration-time data and from the well-stirred liver model [86] suggesting that unbound oral clearance equates to intrinsic clearance under the assumption that the compound is completely absorbed.

For brain penetration in the rat at 2, 6 and 24 h after dosing, male Wistar rats (n = 2) were anaesthetised with 5% isoflurane and sacrificed by opening the diaphragm. A blood sample was taken, plasma was prepared and the brain was slowly perfused with 10 mL 0.9% NaCl solution in water through the carotid. The whole brain was then removed and homogenized in an equal volume of ice-cold 0.1 M Na-phosphate buffer, pH 7.4, using a IKA-WERKE ultra-turrax T25 tissue homogeniser for 10 s, and the brain homogenate was snap frozen in liquid nitrogen. Drug concentrations were then determined as described for plasma, using a calibration curve in blanco brain homogenate.

Notes

The authors declare no competing financial interest.

Acknowledgments

The authors gratefully acknowledge Lucy Baumann, Céline Bortolamiol, Maxime Boucher, Roberto Bravo, Stéphane Delahaye, Alexandre Flock, Elvire Fournier, Hakim Hadana, Julie Hoerner, Benedikt Hofstetter, Niklaus Kuratli, François Le Goff, Claire Maciejasz, Matthias Merrettig, Michel Rauser, Manuela Schläpfer, Virginie Sippel, Daniel Strasser, Gaby von Aesch, René Vogelsanger, Daniel Wanner, Aude Weigel, Rolf Wuest and Nancy Yoganathan for the excellent work and Martine Clozel for support.

Appendix A. Supplementary data

Supplementary data related to this article can be found at <http://dx.doi.org/10.1016/j.ejmech.2016.03.048>.

References

- [1] M. Maceyka, K.B. Harikumar, S. Milstien, S. Spiegel, Sphingosine-1-phosphate signaling and its role in disease, *Trends Cell Biol.* 22 (2012) 50–60.
- [2] T. Mutoh, R. Rivera, J. Chun, Insights into the pharmacological relevance of lysophospholipid receptors, *Br. J. Pharmacol.* 165 (2012) 829–844.
- [3] K. Takabe, S.W. Paugh, S. Milstien, S. Spiegel, “Inside-Out” signaling of sphingosine-1-phosphate: therapeutic targets, *Pharmacol. Rev.* 60 (2008) 181–195.
- [4] J. Rivera, R.L. Proia, A. Olivera, The alliance of sphingosine-1-phosphate and its receptors in immunity, *Nat. Rev. Immunol.* 8 (2008) 753–763.
- [5] C.A. Oskeritzian, S. Milstien, S. Spiegel, Sphingosine-1-phosphate in allergic responses, asthma and anaphylaxis, *Pharmacol. Ther.* 115 (2007) 390–399.
- [6] N.J. Pyne, S. Pyne, Sphingosine 1-phosphate and cancer, *Nat. Rev. Cancer* 10 (2010) 489–503.
- [7] N.J. Pyne, G. Dubois, S. Pyne, Role of sphingosine 1-phosphate and lysophosphatidic acid in fibrosis, *Biochim. Biophys. Acta* 1831 (2012) 228–238.
- [8] Y. Okamoto, F. Wang, K. Yoshioka, N. Takuwa, Y. Takuwa, Sphingosine-1-phosphate-specific G protein-coupled receptors as novel therapeutic targets for atherosclerosis, *Pharmacol. Ther.* 115 (2011) 117–137.
- [9] M. Ishii, J.G. Egen, F. Klauschen, M. Meier-Schellersheim, Y. Saeki, J. Vacher, R.L. Proia, R.N. Germain, Sphingosine-1-phosphate mobilizes osteoclast precursors and regulates bone homeostasis, *Nature* 458 (2009) 524–528.
- [10] T. Baumruker, A. Billich, Sphingolipids in cell signalling: their function as receptor ligands, second messengers, and raft constituents, *Curr. Immunol. Rev.* 2 (2006) 101–118.
- [11] S.E. Alvarez, S. Milstien, S. Spiegel, Autocrine and paracrine roles of sphingosine-1-phosphate, *Trends Endocrinol. Metab.* 18 (2007) 300–307.

- [12] S. Spiegel, S. Milstien, Sphingosine-1-phosphate: an enigmatic signalling lipid, *Nat. Rev. Mol. Cell. Biol.* 4 (2003) 397–407.
- [13] H. Zhang, N.N. Desai, A. Olivera, T. Seki, G. Brooker, S. Spiegel, Sphingosine 1-phosphate, a novel lipid, involved in cellular proliferation, *J. Cell Biol.* 114 (1991) 155–167.
- [14] M. Schuchardt, M. Tölle, J. Prüfer, M. Giet, Pharmacological relevance and potential of sphingosine 1-phosphate in the vascular system, *Br. J. Pharmacol.* 163 (2011) 1140–1162.
- [15] S. Spiegel, S. Milstien, The outs and the ins of sphingosine-1-phosphate in immunity, *Nat. Rev. Immunol.* 11 (2011) 403–415.
- [16] H. Chi, Sphingosine-1-phosphate and immune regulation: trafficking and beyond, *Trends Pharmacol. Sci.* 32 (2011) 16–24.
- [17] H. Rosen, E.J. Goetzl, Sphingosine 1-phosphate and its Receptors: an autocrine and paracrine network, *Nat. Rev. Immunol.* 5 (2005) 560–570.
- [18] J.G. Cyster, Chemokines, sphingosine-1-phosphate and cell migration in secondary lymphoid organs, *Annu. Rev. Immunol.* 23 (2005) 127–159.
- [19] T. Hla, V. Brinkmann, Sphingosine 1-phosphate (S1P) Physiology and the effects of S1P receptor modulation, *Neurology* 76 (2011) S3–S8.
- [20] T. Hla, Physiological and pathological actions of sphingosine 1-phosphate, *Semin. Cell. Dev. Biol.* 15 (2004) 513–520.
- [21] J. Chun, E.J. Goetzl, T. Hla, Y. Garashi, K.R. Lynch, W. Moolenaar, S. Pyne, G.O. Tigyi, International union of pharmacology. XXXIV. Lysophospholipid receptor nomenclature, *Pharmacol. Rev.* 54 (2002) 265–269.
- [22] J.G. Cyster, S.R. Schwab, Sphingosine-1-phosphate and lymphocyte egress from lymphoid organs, *Annu. Rev. Immunol.* 30 (2012) 69–94.
- [23] C.S. Garris, V.A. Blaho, T. Hla, H. M., T. Haaf, Sphingosine-1-phosphate receptor 1 signalling in T cells: trafficking and beyond, *Immunology* 142 (2014) 347–353.
- [24] O.J. David, J.M. Kovarik, R.L. Schmouder, Clinical pharmacokinetics of fingolimod, *Clin. Pharmacokinet.* 51 (2012) 15–28.
- [25] S. Mandala, R. Hajdu, J. Bergstrom, E. Quackenbush, J. Xie, J. Milligan, R. Thornton, G.-J. Shei, D. Card, C. Keohane, M. Rosenbach, J. Hale, C.L. Lynch, K. Rupprecht, W. Parsons, H. Rosen, Alteration of lymphocyte trafficking by sphingosine-1-phosphate receptor agonists, *Science* 296 (2002) 346–349.
- [26] V. Brinkmann, M.D. Davis, C.E. Heise, R. Albert, S. Cottens, R. Hof, C. Bruns, E. Prieschl, T. Baumruker, P. Hiestand, C.A. Foster, M. Zollinger, K.R. Lynch, The immune modulator FTY720 targets sphingosine 1-phosphate receptors, *J. Biol. Chem.* 277 (2002) 21453–21457.
- [27] S.R. Schwab, J.G. Cyster, Finding a way out: lymphocyte egress from lymphoid organs, *Nat. Immunol.* 8 (2007) 1295–1301.
- [28] J. Chun, V. Brinkmann, A mechanistically novel, first oral therapy for multiple sclerosis: the development of fingolimod (FTY720, Gilenya), *Discov. Med.* 64 (2011) 213–228.
- [29] M. Matloubian, C.G. Lo, G. Cinamon, M.J. Lesneski, Y. Xu, V. Brinkmann, M.L. Allende, R.L. Proia, J.G. Cyster, Lymphocyte egress from thymus and peripheral lymphoid organs is dependent on S1P receptor 1, *Nature* 427 (2004) 355–360.
- [30] J.J. Hale, G. Doherty, L. Toth, S.G. Mills, R. Hajdu, C.A. Keohane, M. Rosenbach, J. Milligan, G.-J. Shei, G. Chrebet, J. Bergstrom, D. Card, M. Forrest, S.-Y. Sun, S. West, H. Xie, N. Nomura, H. Rosen, S. Mandalab, Selecting against S1P3 enhances the acute cardiovascular tolerability of 3-(N-benzyl)amino-propylphosphonic acid S1P receptor agonists, *Bioorg. Med. Chem. Lett.* 14 (2004) 3501–3505.
- [31] V. Brinkmann, J.G. Cyster, T. Hla, FTY720: sphingosine 1-phosphate receptor-1 in the control of lymphocyte egress and endothelial barrier function, *Am. J. Transpl. 4* (2004) 1019–1025.
- [32] K. Chiba, Sphingosine 1-phosphate receptor type 1 as a novel target for the therapy of autoimmune diseases, *Inflamm. Regen.* 30 (2010) 160–168.
- [33] D.J. Buzard, J. Thatte, M. Lerner, J. Edwards, R.M. Jones, Recent progress in the development of selective S1P1 receptor agonists for the treatment of inflammatory and autoimmune disorders, *Expert Opin. Ther. Pat.* 18 (2008) 1141–1159.
- [34] M.H. Bolli, C. Lescop, O. Nayler, Synthetic sphingosine 1-phosphate receptor modulators - opportunities and potential pitfalls, *Curr. Top. Med. Chem.* 11 (2013) 726–757.
- [35] E. Roberts, M. Guerrero, M. Urbano, H. Rosen, Sphingosine 1-phosphate receptor agonists: a patent review (2010–2012), *Expert Opin. Ther. Pat.* 23 (2013) 817–841.
- [36] V. Brinkmann, FTY720 (fingolimod) in Multiple Sclerosis: therapeutic effects in the immune and the central nervous system, *Br. J. Pharmacol.* 158 (2009) 1173–1182.
- [37] R.P. Coelho, H.S. Saini, C. Sato-Bigbee, Sphingosine-1-phosphate and oligodendrocytes: from cell development to the treatment of multiple sclerosis, *Prostagl. Other Lipid Mediat.* 91 (2010) 139–144.
- [38] J.W. Choi, S.E. Gardell, D.R. Herr, R. Rivera, C.-W. Lee, K. Noguchi, S.T. Teo, Y.C. Yung, M. Lu, G. Kennedy, J. Chun, FTY720 (fingolimod) efficacy in an animal model of multiple sclerosis requires astrocyte sphingosine 1-phosphate receptor 1 (S1P1) modulation, *Proc. Natl. Acad. Sci. U.S.A.* 108 (2011) 751–756.
- [39] A. Groves, Y. Kihara, J. Chun, Fingolimod: direct CNS effects of sphingosine 1-phosphate (S1P) receptor modulation and implications in multiple sclerosis therapy, *J. Neurol. Sci.* 328 (2013) 9–18.
- [40] M. Forrest, S.-Y. Sun, R. Hajdu, J. Bergstrom, D. Card, G. Doherty, J. Hale, C. Keohane, C. Meyers, J. Milligan, S. Mills, N. Nomura, H. Rosen, M. Rosenbach, G.-J. Shei, I.I. Singer, M. Tian, S. West, V. White, J. Xie, R.L. Proia, S. Mandala, Immune cell regulation and cardiovascular effects of sphingosine 1-phosphate receptor agonists in rodents are mediated via distinct receptor subtypes, *JPET* 309 (2004) 758–768.
- [41] M.G. Sanna, J. Liao, E. Jo, C. Alfonso, M.-Y. Ahn, M.S. Peterson, B. Webb, S. Lefebvre, J. Chun, N. Gray, H. Rosen, Sphingosine 1-phosphate (S1P) receptor subtypes S1P1 and S1P3, respectively, regulate lymphocyte recirculation and heart rate, *J. Biol. Chem.* 279 (2004) 13839–13848.
- [42] S. Salomone, E. Potts, S. Tyndall, P. Ip, J. Chun, V. Brinkmann, C. Waeber, Analysis of sphingosine 1-phosphate receptors involved in constriction of isolated cerebral arteries with receptor null mice and pharmacological tools, *Br. J. Pharmacol.* 153 (2007) 1–8.
- [43] A. Murakami, H. Takasugi, S. Ohnuma, Y. Koide, A. Sakurai, S. Takeda, T. Hasegawa, J. Sasamori, T. Konno, K. Hayashi, Y. Watanabe, Y.S. Koji Mori, A. Takahashi, N. Mochizuki, N. Takakura, Sphingosine 1-phosphate (S1P) regulates vascular contraction via S1P3 receptor: investigation based on a new S1P3 receptor antagonist, *Mol. Pharmacol.* 77 (2010) 704–713.
- [44] R.M. Fryer, A. Muthukumarana, P.C. Harrison, S.N. Mazurek, R.R. Chen, K.E. Harrington, R.M. Dinallo, J.C. Horan, L. Patnaude, L.K. Modis, G.A. Reinhart, The clinically-tested S1P receptor agonists, FTY720 and BAF312, demonstrate subtype-specific bradycardia (S1P1) and hypertension (S1P3) in rat, *PLoS One* 7 (2012) e52985.
- [45] L.M. Healy, J.P. Antel, Sphingosine-1-phosphate receptors in the central nervous and immune systems, *Curr. Drug Targets* 17 (2016) 1–10.
- [46] S. Crosignani, A. Bombrun, D. Covini, M. Maio, D. Marin, A. Quattropiani, D. Swinnen, D. Simpson, W. Sauer, B. Françon, T. Martin, Y. Cambet, A. Nichols, I. Martinou, F. Burgat-Charvillon, D. Rivron, C. Donini, O. Schott, V. Eligert, L. Novo-Perez, P.-A. Vitte, J.-F. Arrighi, Discovery of a novel series of potent S1P1 agonists, *Bioorg. Med. Chem. Lett.* 20 (2010) 1516–1519.
- [47] M.H. Bolli, S. Abele, C. Binkert, R. Bravo, S. Buchmann, D. Bur, J. Gatfield, P. Hess, C. Kohl, C. Mangold, B. Mathys, K. Menyhart, C. Mueller, O. Nayler, M. Scherz, G. Schmidt, V. Sippel, B. Steiner, D. Strasser, A. Treiber, T. Weller, 2-Imino-thiazolidin-4-one derivatives as potent, orally active S1P1 receptor agonists, *J. Med. Chem.* 53 (2010) 4198–4211.
- [48] E.H. Demont, B.I. Andrews, R.A. Bit, C.A. Campbell, J.W.B. Cooke, N. Deeks, S. Desai, S.J. Dowell, P. Gaskin, J.R.J. Gray, A. Haynes, D.S. Holmes, U. Kumar, M.A. Morse, G.J. Osborne, T. Panchal, B. Patel, A. Perboni, S. Taylor, R. Watson, J. Witherington, R. Willis, Discovery of a selective S1P1 receptor agonist efficacious at low oral dose and devoid of effects on heart rate, *Med. Chem. Lett.* 2 (2011) 444–449.
- [49] H. Kurata, K. Kusumi, K. Otsuki, R. Suzuki, M. Kurono, N. Tokuda, Y. Takada, H. Shioya, H. Mizuno, T. Komiya, T. Ono, H. Hagiya, M. Minami, S. Nakade, H. Habashita, Structure–activity relationship studies of S1P agonists with a dihydronaphthalene scaffold, *Bioorg. Med. Chem. Lett.* 22 (2012) 144–148.
- [50] D.J. Buzard, S. Han, L. Lopez, A. Kawasaki, J. Moody, L. Thoresen, B. Ullman, J. Lehmann, I. Calderon, X. Zhu, T. Gharbaoui, D. Sengupta, A. Krishnan, Y. Gao, J. Edwards, J. Barden, M. Morgan, K. Usmani, C. Chen, A. Sadeque, J. Thatte, M. Solomon, L. Fu, K. Whelan, L. Liu, H. Al-Shamma, J. Gatlin, M. Le, C. Xing, S. Espinola, R.M. Jones, Fused tricyclic indoles as S1P1 agonists with robust efficacy in animal models of autoimmune disease, *Bioorg. Med. Chem. Lett.* 22 (2012) 4404–4409.
- [51] T. Nakamura, M. Asano, Y. Sekiguchi, Y. Mizuno, K. Tamaki, T. Kimura, F. Nara, Y. Kawase, T. Shimozato, H. Doi, T. Kagari, W. Tomisato, R. Inoue, M. Nagasaki, H. Yuita, K. Oguchi-Oshima, R. Kaneko, N. Watanabe, Y. Abe, T. Nishi, Discovery of CS-2100, a potent, orally active and S1P3-sparing S1P1 agonist, *Bioorg. Med. Chem. Lett.* 22 (2012) 1788–1792.
- [52] M.S. Freedman, T. Olsson, M. Melanson, Ó. Fernández, A. Boster, D. Bach, O. Berkani, M. Mueller, T. Sidorenko, C. Pozzilli, Dose-dependent effect of ponesimod, an oral, selective sphingosine 1-phosphate receptor-1 modulator, on magnetic resonance imaging outcomes in patients with relapsing–remitting multiple sclerosis, in: 28th European Committee for the Treatment and Research in Multiple Sclerosis (ECTRIMS), 2012. P923.
- [53] S. Pan, N.S. Gray, W. Gao, Y. Mi, Y. Fan, X. Wang, T. Tuntland, J. Che, S. Lefebvre, Y. Chen, A. Chu, K. Hinterding, A. Gardin, P. End, P. Heining, C. Bruns, N.G. Cooke, B. Nuesslein-Hildesheim, Discovery of BAF312 (siponimod), a potent and selective S1P receptor modulator, *Med. Chem. Lett.* 4 (2013) 333–337.
- [54] Receptos, Receptos Reports Positive Phase 2 Results for RPC1063 in Relapsing Multiple Sclerosis, 2014. RCPT_News_2014_6_9_General_Releases.
- [55] M. Bigaud, D. Guerini, A. Billich, F. Bassilana, V. Brinkmann, Second generation S1P pathway modulators: research strategies and clinical developments, *Biochim. Biophys. Acta* 1841 (2013) 745–758.
- [56] P. Brossard, H. Derendorf, J. Xu, H. Maatouk, A. Halabi, J. Dingemans, Pharmacokinetics and pharmacodynamics of ponesimod, a selective S1P receptor modulator, in the first-in-human study, *Br. J. Clin. Pharmacol.* 76 (2013) 888–896.
- [57] P. Gergely, E. Wallström, B. Nuesslein-Hildesheim, C. Bruns, F. Zécúri, N. Cooke, M. Traebert, T. Tuntland, M. Rosenberg, M. Saltzman, Phase I study with the selective S1P1/S1P5 receptor modulator BAF312 indicates that S1P1 rather than S1P3 mediates transient heart rate reduction in humans, in: 25th Congress of the European Committee for the Treatment and Research in Multiple Sclerosis (ECTRIMS), 2009. P437.
- [58] P. Gergely, B. Nuesslein-Hildesheim, D. Guerini, V. Brinkmann, M. Traebert, C. Bruns, S. Pan, N.S. Gray, K. Hinterding, N.G. Cooke, A. Groenewegen, A. Vitaliti, T. Sing, O. Luttringer, J. Yang, A. Gardin, N. Wang, W.J. Crumb Jr., M. Saltzman, M. Rosenberg, E. Wallstrom, The selective sphingosine 1-

- phosphate receptor modulator BAF312 redirects lymphocyte distribution and has species-specific effects on heart rate, *Br. J. Pharmacol.* 167 (2012) 1035–1047.
- [59] M.H. Bolli, S. Abele, M. Birker, R. Bravo, D. Bur, R. De Kanter, C. Kohl, J. Grimont, P. Hess, C. Lescop, B. Mathys, C. Müller, O. Nayler, L. Piali, M. Rey, M. Scherz, G. Schmidt, J. Seifert, B. Steiner, J. Velker, T. Weller, Novel S1P1 receptor agonists – part 3: from thiophenes to pyridines, *J. Med. Chem.* 57 (2014) 110–130.
- [60] H. Spielmann, M. Balls, J. Dupuis, W.J. Pape, G. Pechovitch, O. de Silva, H.-G. Holzhütter, R. Clothier, P. Desolle, F. Gerberick, M. Liebsch, W.W. Lovell, T. Maurer, U. Pfannenbecker, J.M. Potthast, M. Csato, D. Sladowski, W. Steiling, P. Brantom, The international EU/COLIPA *in vitro* phototoxicity validation study: results of the phase II (blind trial). Part1: the 3T3 NRU phototoxicity test, *Toxicol. In Vitro* 12 (1998) 305–327.
- [61] B. Peters, H.-G. Holzhütter, *In vitro* phototoxicity testing: development and validation of a new concentration response analysis software and biostatistical analyses related to the use of various prediction models, *ATLA* 30 (2002) 415–432.
- [62] A.M. Lynch, P. Wilcox, Review of the performance of the 3T3 NRU *in vitro* phototoxicity assay in the pharmaceutical industry, *Exp.Toxicol. Pathol.* 63 (2011) 209–214.
- [63] S. Onoue, N. Igarashi, Y. Yamauchi, T. Kojima, N. Murase, Y. Zhou, S. Yamada, Y. Tsuda, *In vitro* phototoxic potential and photochemical properties of imidazopyridine derivative: a novel 5-HT4 partial agonist, *J. Pharm. Sci.* 97 (2008) 4307–4318.
- [64] M.D. Barratt, Structure-activity relationship and prediction of the phototoxicity and phototoxic potential of new drugs, *ATLA* 32 (2004) 511–524.
- [65] M.H. Bolli, C. Müller, B. Mathys, S. Abele, M. Birker, R. Bravo, D. Bur, P. Hess, C. Kohl, D. Lehmann, O. Nayler, M. Rey, S. Meyer, M. Scherz, G. Schmidt, B. Steiner, A. Treiber, J. Velker, T. Weller, Novel S1P1 receptor agonists – part 1: from pyrazoles to thiophenes, *J. Med. Chem.* 56 (2013) 9737–9755.
- [66] M.H. Bolli, J. Velker, C. Müller, B. Mathys, M. Birker, R. Bravo, D. Bur, R. d. Kanter, P. Hess, C. Kohl, D. Lehmann, S. Meyer, O. Nayler, M. Rey, M. Scherz, B. Steiner, Novel S1P1 receptor agonists – part 2: from bicyclo[3.1.0]hexane-fused thiophenes to isobutyl substituted thiophenes, *J. Med. Chem.* 57 (2014) 78–97.
- [67] W. Buratti, G.P. Gardini, F. Minisci, Nucleophilic character of alkyl radicals-V Selective homolytic alpha-oxyalkylation of heteroaromatic bases, *Tetrahedron* 27 (1971) 3655–3688.
- [68] M.H. Bolli, C. Lescop, B. Mathys, C. Mueller, O. Nayler, B. Steiner, Novel Aminomethyl Benzene Derivatives. WO2009109904, Sep. 11, 2009.
- [69] Mihara, J.; Murata, T.; Yamazaki, D.; Yoneta, Y.; Shibuya, K.; Shimojo, E.; Görgens, U.; Turberg, A.; Bach, T. Insecticidal aryl isoxazoline derivatives. US2010/0179194 A1, Jul 15, 2010.
- [70] G. Costantino, M. Marinozzi, E. Camaioni, N. Natalini, I. Sarichelou, F. Micheli, P. Cavanni, S. Faedo, C. Noe, F. Moroni, R. Pellicciari, Stereoselective synthesis and preliminary evaluation of (+)- and (-)-3-methyl-5-carboxy-thien-2-ylglycine (3-MATIDA): identification of (+)-3-MATIDA as a novel mGluR1 competitive antagonist, *Il Farm.* 59 (2004) 93–99.
- [71] M.H. Bolli, C. Lescop, B. Mathys, C. Mueller, O. Nayler, B. Steiner, Novel Thiophene Derivatives. WO2009074950, June 18, 2009.
- [72] R.S. Obach, Prediction of human clearance of twenty-nine drugs from hepatic microsomal intrinsic clearance data: an examination of the *in vitro* half-life approach and nonspecific binding to microsomes, *Drug Metab. Dispos.* 27 (1999) 1350–1359.
- [73] R.P. Austin, P. Barton, S.L. Cockroft, M.C. Wenlock, R.J. Riley, The influence of nonspecific microsomal binding on apparent intrinsic clearance, and its prediction from physicochemical properties, *Drug Metab. Dispos.* 33 (2002) 1497–1503.
- [74] M.J. Sykes, M.J. Soric, J.O. Miners, Molecular modeling approaches for the prediction of the nonspecific binding of drugs to hepatic microsomes, *J. Chem. Inf. Model.* 46 (2006) 2661–2673.
- [75] X. Liu, M. Wright, C.E.C.A. Hop, Rational use of plasma protein and tissue binding data in drug design, *J. Med. Chem.* 57 (2014) 8238–8248.
- [76] J. Wagner, P.v. Matt, B. Faller, N.G. Cooke, R. Albert, R. Sedrani, H. Wiegand, C. Jean, C. Beerli, G. Weckbecker, J.-P. Ewenou, G. Zenke, S. Cottens, Structure-activity relationship and pharmacokinetic studies of sotrastaurin (AEB071), a promising novel medicine for prevention of graft rejection and treatment of psoriasis, *J. Med. Chem.* 54 (2011) 6028–6039.
- [77] N.J. Abbott, D.E.M. Dolman, A.K. Patabendige, Assays to predict drug permeation across the blood-brain barrier, and distribution to brain, *Curr. Drug Metab.* 9 (2008) 901–910.
- [78] T.T. Wager, A. Villalobos, P.R. Verhoest, X. Hou, C.L. Shaffer, Strategies to optimize the brain availability of central nervous system drug candidates, *Exp. Op. Drug Disc.* 6 (2011) 371–381.
- [79] T.T. Wager, R.Y. Chandrasekaran, X. Hou, M.D. Troutman, P.R. Verhoest, A. Villalobos, Y. Will, Defining desirable central nervous system drug space through the alignment of molecular properties, *in vitro* ADME, and safety attributes, *ACS Chem. Neurosci.* 1 (2010) 420–434.
- [80] T.T. Wager, X. Hou, P.R. Verhoest, A. Villalobos, Moving beyond rules: the development of a central nervous system multiparameter optimization (CNS MPO) approach to enable alignment of druglike properties, *ACS Chem. Neurosci.* 1 (2010) 435–449.
- [81] E. Baciocchi, T.D. Giacco, A. Lapi, Oxygenation of benzyldimethylamine by singlet oxygen. Products and mechanism, *Org. Lett.* 6 (2004) 4791–4794.
- [82] E. Baciocchi, T.D. Giacco, O. Lanzalunga, A. Lapi, Singlet oxygen promoted carbon-heteroatom bond cleavage in dibenzyl sulfides and tertiary dibenzylamines. Structural effects and the role of exciplexes, *J. Org. Chem.* 72 (2007) 9582–9589.
- [83] M.H. Bolli, C. Lescop, M. Birker, R.d. Kanter, P. Hess, C. Kohl, O. Nayler, M. Rey, P. Sieber, J. Velker, T. Weller, B. Steiner, Novel S1P1 receptor agonists – Part 5: from amino-to alkoxy-pyridines, *Eur. J. Med. Chem.* 115 (2016) 326–341.
- [84] J. Grimont, F. Le Goff, G. Bourquin, J. Silva, Quality assessment and concentration determination of Actelion's compound solutions by automated LCMS and quantitative NMR, in: MipTec 2010-The Leading European Event for Drug Discovery, Basel, Switzerland, Sep 20–24, 2010.
- [85] R.S. Obach, A.E. Reed-Hagen, Measurement of Michaelis constants for cytochrome P450-mediated biotransformation reactions using a substrate depletion approach, *Drug Metab. Dispos.* 30 (2002) 831–837.
- [86] M. Rowland, L.Z. Benet, G.G. Graham, Clearance concepts in pharmacokinetics, *J. Pharmacokinet. Pharmacodyn.* 1 (1973) 123–136.